WL-TM-92-332

Hydrodynamic Investigation of Vortical Flows for an ATTAC Configuration with Canards

Lawrence W. Rogers
Capt Michael G. Alexander

WL/FIMM
Aeromechanics Division

June 1992

Original contains color plates: All DTIC reproductions will be in black and white

FLIGHT DYNAMICS DIRECTORATE
WRIGHT LABORATORY
AIR FORCE SYSTEMS COMMAND
WRIGHT-PATTERSON AIR FORCE BASE, OH 45433-6553

REPORT DOCUMENTATION PAGE

Form Approved
OMB No. 0704-0188

1. AGENCY USE ONLY *(Leave blank)*	2. REPORT DATE	3. REPORT TYPE AND DATES COVERED
	Jun 92	TM-Oct 90-Dec 91

4. TITLE AND SUBTITLE
Hydrodynamic Investigation of Vortical Flows for an ATTAC Configuration with Canards

5. FUNDING NUMBERS
240410B2

6. AUTHOR(S)
Lawrence W. Rogers
Capt Michael G. Alexander

7. PERFORMING ORGANIZATION NAME(S) AND ADDRESS(ES)
WL/FIMM
Aeromechanics Division
Flight Dynamics Directorate
Wright Laboratory
Wright-Patterson AFB OH 45433-6553

8. PERFORMING ORGANIZATION REPORT NUMBER
WL-TM-92-332

9. SPONSORING/MONITORING AGENCY NAME(S) AND ADDRESS(ES)
WL/FIMM
Aeromechanics Division
Flight Dynamics Directorate
Wright Laboratory
Wright-Patterson AFB OH 45433-6553

10. SPONSORING/MONITORING AGENCY REPORT NUMBER
WL-TM-92-332

11. SUPPLEMENTARY NOTES
N/A

12a. DISTRIBUTION/AVAILABILITY STATEMENT
Approved for public release; distribution unlimited

12b. DISTRIBUTION CODE

13. ABSTRACT *(Maximum 200 words)*

Hydrodynamic investigation was conducted on an ATTAC Fighter model to qualitatively determine the nature of forebody/Canard/LEX/wing vortex systems. Dye flow visualization was accomplished for angles of attack from 5 to 40 degrees and Canard deflections from +10 to -20 degrees. A Canard Deflection of -10 degrees created least disturbance to the vortex systems.

14. SUBJECT TERMS
Vortex Flow, Hydrodynamic Testing, Flow Visualization, Canard Effectiveness

15. NUMBER OF PAGES
44

16. PRICE CODE

17. SECURITY CLASSIFICATION OF REPORT	18. SECURITY CLASSIFICATION OF THIS PAGE	19. SECURITY CLASSIFICATION OF ABSTRACT	20. LIMITATION OF ABSTRACT
Unclassified	Unclassified	Unclassified	DTIC Users

Abstract

A water tunnel investigation was conducted on a 2% scale Advanced Technologies for Tactical Aircraft (ATTAC) fighter model at Wright Laboratory's 2ft Hydrodynamic Facility at Wright-Patterson AFB, Ohio. This investigation focused on qualitatively establishing vortex systems, trajectories, and paths. The water tunnel test matrix was conducted at a Reynolds number per foot of approximately 28,000. Dye flow visualization was accomplished for angles-of-attack from $+5^{o}$ to $+40^{o}$, sideslips -5^{o} to $+10^{o}$ and canards angles of $+10^{o}$ to -20^{o}.

The canards were shown to be effective vortex management devices in this water tunnel investigation with a deflection of -10^{o} creating least disturbance to the forebody/LEX/wing vortex systems. Flow visualization offered vivid evidence of the LEX vortex persistence.

Foreword

This technical memorandum was prepared by Mr. Lawrence W. Rogers and Captain Michael G. Alexander . This report documents a water tunnel test conducted by the Airframe Aerodynamics Group, Aeromechanics Division, Flight Dynamics Directorate, Wright-Patterson AFB, 45433-6553. This work was performed in October 1990 and December 1991 under project 240410B2, Vortex Flow Technology.

The authors wish to thank Mr. Dick Heck and Airman Doug Barton for their help and expertise during the testing.

This report has been reviewed and is approved.

Lawrence W. Rogers
Aerospace Engineer
Airframe Aerodynamics Group

Michael G. Alexander, Captain,USAF
Aerospace Engineer
Airframe Aerodynamics Group

Russell F. Osborn
Technical Manager
Airframe Aerodynamics Group

Dennis Sedlock
Chief
Aerodynamics and Airframe Branch

Table of Contents

List of Figures

I Introduction

This investigation of vortical flow was initiated by the The Technical Cooperation Program (TTCP), Subgroup H, Aeronautics Technology Technical Panel, HTP-5, Maneuvering Aerodynamics Group. The TTCP is an international cooperative program that includes members from the United States, United Kingdom, Australia, Canada, and New Zealand that fosters gathering of technical information and exchange. Within the HTP-5 group, a collaborativeprogram was established with the United States and the United Kingdom to investigate the control of vortical flow by canard surfaces.

The fighter configuration provided for this research activity was the Advanced Technologies for Tactical Aircraft (ATTAC) supersonic STOL-capable fighter concept that was used during the early 1980's. This canard configuration was a dual role tactical fighter aircraft concept embodying a technology complement of the 1980's.

The water tunnel test was in support and accomplished after the wind tunnel test. The purpose of the water tunnel test was to visualize and give insight into the vortex systems and establish their paths and trajectories. This test is purely qualitative due to the low Reynolds number which contributed to a laminar boundary layer. However, at angles-of-attack greater than 10^{o} (reference 2), it has been demonstrated that water tunnel results correlate well to flight test results, especially with slender swept canard/wing configurations.

In a viscous fluid, vorticity is transported by convection and diffusion. At high Reynolds numbers, a significant difference in the scale of the two transport processes exists, the ratio of the scales of diffusion and convection being on the order of $1/Re^{1/2}$. The latter term is also a measure of the boundary layer thickness. The rate of expansion of the vortex with distance 'x' along the axis is of the order l/x, where 'l' is the lateral scale or "diameter" of the large-scale structure of the vortex. In vortices studied experimentally, l/x is typically much greater than $1/Re^{1/2}$. In water tunnel studies for a 0.305-meter slender wing at $\alpha = 20^{o}$, l/x at the trailing edge is approximately 0.24 whereas $1/Re^{1/2} = 0.006$. Consequently, even at the low Reynolds numbers typical of water tunnels, the condition that $l/x >> 1/Re^{1/2}$ is generally satisfied, meaning the size of the vortex is much

greater than the undisturbed boundary layer thickness. It appears that, in these cases, the large scale vortex structure must have been determined primarily by the convection transport mechanism and is likely to have been largely independent of Reynolds numbers.

Essentially there are two different vortex regimes:

(1) Viscous vortex submerged or partially submerged in the boundary layer,
(2) Predominantly inviscid vortex, large relative to the local boundary layer thickness,which can be regarded as a vortex sheet subject to relatively minor modification due to viscous diffusion.

In addition to the dominance of diffusion at very low Reynolds numbers, there is also an angle-of-attack range at a given Reynolds number within which the vortices are of the viscous type. As a result, a relationship can be envisioned between Reynolds number and angle-of-attack which defines whether a vortex is of the inviscid or viscous type. As a result, water tunnel simulation of vortex flows at low angles-of-attack ($\alpha < 10^{o}$) can be unrepresentative because the vortices are of the viscous type, unlike the inviscid type vortices generally observed at high Reynolds numbers in the wind tunnel or flight. At high angles-of-attack in the water tunnel, the flow field is vortex dominated and, hence, good agreement is observed with high Reynolds number results in air. In general water tunnel experience indicates that the vortex core height above the surface must be of the order of ten boundary layer thicknesses or more in order to be in the inviscid regime in order to apply water tunnel results to wind tunnel and flight results.

II Experimental Apparatus

2.1 Water Tunnel

The Wright Laboratory's 2ft x 2ft Hydrodynamic Facility is located at Wright-Patterson AFB, Ohio, (figure 1) and is a continuous gravity flow tunnel with a maximum velocity of 0.85 ft/s. Optimum dye flow visualization velocities range from 0.1 to 0.3 ft/s. At a velocity of 0.3 ft/s, the average test section centerline turbulence is 7% (ref 3). The test section is 2ft x 2ft and has a length of 4ft. Two-inch thick Plexiglass windows are located in two sides of the water tunnel to allow planform and side view observations. A third side allows model entry.

Testing was performed at a velocity of 0.3 f/s at a Reynolds number per foot of approximately 28,000. Testing parameters were α = + 5^o to +40^o, β = - 5^o to +10^o (Δ 5^o) and α_c = +10^o to -20^o (Δ 10^o). The water tunnel test matrix can be seen in figure 2.

2.2 Water Tunnel Model

Wing	Canard
AR = 3.34	AR = 1.37
Λ_{LE}= 51^o	Λ_{LE}= 50^o
Λ_{LEX}=70^o	b = 10.5 in
L_{fuse}= 18 in	

Dye taps were located on the lower surfaces of the forebody/canard/LEX/wing system close to the leading edges so that the dye would be entrained into the primary vortices. Dye was forced from a containment reservoir to the model using compressed air.

III Analysis

3.1 Water Tunnel

Water tunnel experimentation is considered a credible external flow simulation instrument if certain model and testing guidelines are followed as indicated in reference 2. The most stringent parameter is the model shape itself. Chined forebodies and moderate to highly swept, sharp leading edge wings are paramount considerations since the separation point at the leading edges are not Reynolds number dependent. Another important test consideration is that the vortices should be well established and far enough above the model surface, in the potential flow field, so that the scale (physical size) of the vortex flow is much greater than the undisturbed boundary layer thickness. In other words, water tunnel testing should be at high enough angles-of-attack which result in vortex dominated flow fields (ref 5). Reference 2 indicates that water tunnel testing should be accomplished above 10^{o} in angle-of-attack. In figure 4, the basic ATTAC vortical systems are identified.

3.1.1 $\alpha = 15^{o}$ to 40^{o}; $\beta = 0^{o}$; α_c = Off

The ATTAC water tunnel model with canards removed exhibited a predictable vortex development at $\beta = 0^{o}$ as the angle-of-attack was increased from 5^{o} to 40^{o}. At $\alpha = 15^{o}$ (figure 5), the forebody and the LEX vortices are well established with the wing vortices already exhibiting bursting. By $\alpha = 20^{o}$ (figure 6), the wing vortices are totally burst with the forebody vortices maintaining their structure and being drawn towards their respective wings near the trailing edge. Significantly, as α approaches 35^{o} (figure 7), the forebody/LEX vortex structure remains intact which can be attributed to the LEX's large leading edge sweep angle and also due to the influence of the forebody vortices which have yet to burst. Mention should be made here of the asymmerty in the wing vortex burst locations. This asymmetry is probably due to such factors as slight model asymmetries and the Hydrodynamic facility's test section velocity profile and streamline deviations as seen in reference 3. Figure 8 from reference 4 shows additional vortex bursting asymmetry evidence at $\beta = 0^{o}$ in the same facility.

3.1.2 $\alpha = 15^{o}$ to 30^{o}; $\beta = +5^{o}$; α_c = Off

At $\alpha = 15^{o}$ (figure 9), a β of $+5^{o}$ has an appreciable effect on the vortex system when compared with the unyawed case in figure 5. There is an enhancement/strengthening of the leeward wing/LEX vortices as well as a significant windward forebody vortex movement as evidenced in the sideview in figure 9. As observed in figure 9, the windward forebody vortex has moved upwards and towards the leeward side. This type of movement would result in a change in lateral/directional characteristics of this canardless configuration. The aforementioned enhancement and movement of the vortex system can be attributed to the resultant increases and decreases in the leading edge sweep angles of the forebody/LEX and wing. Also of note, in figure 9 , the asymmetric wing vortex bursting has been exacerbated resulting in increased rolling moment instability. As the model was pitched to $\alpha = 20^{o}$ and 30^{o} (figures 10 and 11), the leeward forebody vortex has migrated towards the leeward wing vortex which has totally burst. This in effect increases the forebody vortex asymmetry in the empennage area directly influencing the lateral/directional stability. Even though, at these moderate to high angles-of-attack with the wing vortices completely burst and the forebody vortices migrating considerably, the LEX vortices remain intact.

3.1.3 $\alpha = 15^{o}$ to 35^{o}; $\beta = 0^{o}$; α_c = On

Section 3.1.1 and 3.1.2 have discussed the hydrodynamic test of the ATTAC model with the canard off. Now a qualitative analysis will be accomplished with canards on at deflection angles (α_c) of 0^{o}, -10^{o}, -20^{o}, and $+10^{o}$. Figure 12 shows a well defined forebody/canard/LEX/wing vortex system. Bursting is evident on the wings and canards as shown in the planform and sideviews for $\alpha_c = 0^{o}$ and $\alpha = 15^{o}$. Note how the wing's leading edge vortex has coupled with the LEX's vortex and has become one vortex system and how the forebody vortex has migrated onto the left wing. At $\alpha = 20^{o}$ (figure 13 and 30^{o} (figure 14), it's apparent that the burst canard vortices have caused a flow field disturbance and altered the forebody vortices trajectories while the LEX vortices remain intact. Note that almost total bursting has occurred on the wings. When the canards are deflected to $\alpha_c = -10^{o}$ at $\alpha = 15^{o}$ (figure 15), the canards seem to cause less disturbance on the LEX/wing vortex system when compared with the canard deflected at $\alpha_c = 0^{o}$ at the same angle-of-attack (figure 12). As the model is pitched to $\alpha = 18^{o}$

(figure 16) and $\alpha = 25^{o}$ (figure 17), this trend of less disturbance/interaction from the canards continues allowing for a more stable LEX/wing vortex system than that which occurred at $\alpha_c = 0^{o}$. Due to the less disturbance/interaction created by the canards, it is apparent that vortex bursting has been delayed on the wings and occurs nearer to the wing trailing edges. Vortex bursting on the canards is also delayed which lessens the interference effects on the forebody vortices. In figure 17, an asymmetric wing vortex bursting is observed which would result in an increased rolling moment. This asymmetry, at $\beta = 0^{o}$, was also noted in section 3.1.1 with the canards removed. As angle-of-attack increase from $\alpha = 25^{o}$ to $\alpha = 35^{o}$ (figure 18), the canards and wing vortices have totally burst, whereas the forebody/LEX vortex system remains essentially intact.

In figure 19 ($\alpha = 15^{o}$, $\beta = 0^{o}$, $\alpha_c = -20^{o}$), it's apparent that leading edge vortex flow is not established on the canards since they are at an angle-of-attack (α_g) of -5 degrees. The forebody/LEX/wing vortex system is relatively undisturbed, while the previously discussed wing vortex asymmetric burst location remains. However, as α is increased to 25^{o} and 30^{o} (figures 20 & 21), the LEX vortices' path has been altered due to decreased vortical strength which is due to the canard upwash interacting with the LEX's flow field. The wing vortices have totally burst. Comparing figure 20 to figure 17 ($\alpha_c = -10^{o}$), the comparison indicates that $\alpha_c = -20^{o}$ causes more wing bursting and LEX interaction.

With the canards deflected upwards to $\alpha_c = +10^{o}$ ($\alpha = +15^{o}$, $\beta = 0^{o}$), figure 22 shows the canards have completely stalled with the leading edge vortices completely burst since the canards are at an angle-of-attack (α_g) of $+25^{o}$. The LEX vortices once again exhibit reduced strength and an altered path. At this configuration, this flow activity would certainly translate to a longitudinal stability change since the canard/LEX vortex system has been altered. A positive canard setting would probably be effective in controlling a pitch up problem by controlling the canard/LEX vortices.

5.1.4 $\alpha = 15^{o}$ to 30^{o}; $\beta = +5^{o}, +10^{o}$; $\alpha_c = -10^{o}$

In figure 23, ($\alpha = 15^{o}$, $\beta = +5^{o}$, $\alpha_c = -10^{o}$), the leeward canard/LEX/wing vortex system has increased in strength due to the increase in leading edge sweep angles of these components. This figure clearly shows that the windward forebody vortex has migrated

towards the leeward side and the sideview indicates this same vortex has moved upwards away from the surface. The result of this vortex strengthening/movement would exhibit itself in lateral/directional stability changes. As α increases to 20^{o} (figure 24) and 30^{o} (figure 25), it's evident that there is an increased asymmetry in the canard/wing burst locations. This type of asymmetry will give rise to an increased rolling moment instability. There is also a pronounced lateral migration of the forebody vortices as well as in increased trajectory asymmetry. Up to $\alpha = 30^{o}$, the LEX vortices maintain structure, especially on the leeward side.

In figure 26, ($\alpha = 15^{o}$, $\beta = +10^{o}$, $\alpha_{c} = -10^{o}$), the additional 5 degrees of sideslip can be seen in the strengthening of the leeward canard/LEX/wing vortices. Also, the forebody vortex migration has increased as well as more detrimental wing vortex bursting asymmetry. This trend can be seen in figure 27 ($\alpha = 18^{o}$), figure 28 ($\alpha = 25^{o}$), and figure 29 ($\alpha = 30^{o}$). Obviously, wing bursting asymmetry as well as migration of the windward forebody vortex to the leeward side would result in an increased lateral/directional stability problems. The forebody/LEX vortex system, at $\alpha = 25^{o}$ and 30^{o}, is maintaining its structure while the wing vortices have almost completely burst. A change in longitudinal stability could be expected.

IV Recommendations and Conclusions

1 - The canards behaved as effective vortex management devices in this hydrodynamic test with $\alpha_c = -10^o$ creating less disturbance to the forebody/LEX/wing vortex systems.

2 - Canard deflections of -20^o and $+10^o$ caused more interactions with the forebody/LEX vortex system than any other deflections.

3 - Flow visualization offered vivid evidence of possible effects of asymmetric wing bursting, forebody vortex trajectory changes, and LEX vortex persistence.

4 - Water tunnels give acceptable qualitative results when compared to wind tunnel and flight tests if the vortex core is approximately 10 boundary layer thicknesses above the surface (typically $\alpha > +10^o$).

5 - Recommend model spanwise pressure taps, flow visualization and higher angles-of-attack for fully developed vortex behavior and interactions for any further higher Reynolds number wind tunnel testing.

V List of References

1) Krepski, R.E., Hendrickson, R.H., Investigation of Advanced Technologies for Tactical Aircraft, Volume IV, Parts I & II, Flight Dynamics Laboratory, Wright-Patterson AFB, Ohio, 45433, AFWAL-TR-82-3069, DTIC - AD B079145 & AD B079146, Aug. 1983.

2) Erickson, Gary E., Vortex Flow Correlation, Flight Dynamics Laboratory, Wright-Patterson AFB, Ohio 45433, AFWAL-TR-80-3142, Jan. 1981.

3) Heck, R., Rogers, L, Large Hydrodynamic Tunnel Calibration Recommendation for Quality Improvement, Flight Dynamics Laboratory, Wright-Patterson AFB, Ohio, 45433, WRDC-TM-168, May 1989.

4) LeMay, S.P., Vortex Flow Visualization Using Colored and Fluorescent Dyes on a Flat Plate Wing with Leading Edge Extension. A Water Tunnel Study, Flight Dynamics Directorate, Wright-Patterson AFB, Ohio, 45433, WL-TM-92-323, May 1992.

5) Rogers, L.W., Water/Wind Tunnel Test of a Generic Fighter Aerodynamic Development Aircraft - Vortex Flow Visualization, Flight Dynamics Laboratory, Wright-Patterson AFB, Ohio, 45433, WRDC-TM-89-171, Sept. 1989.

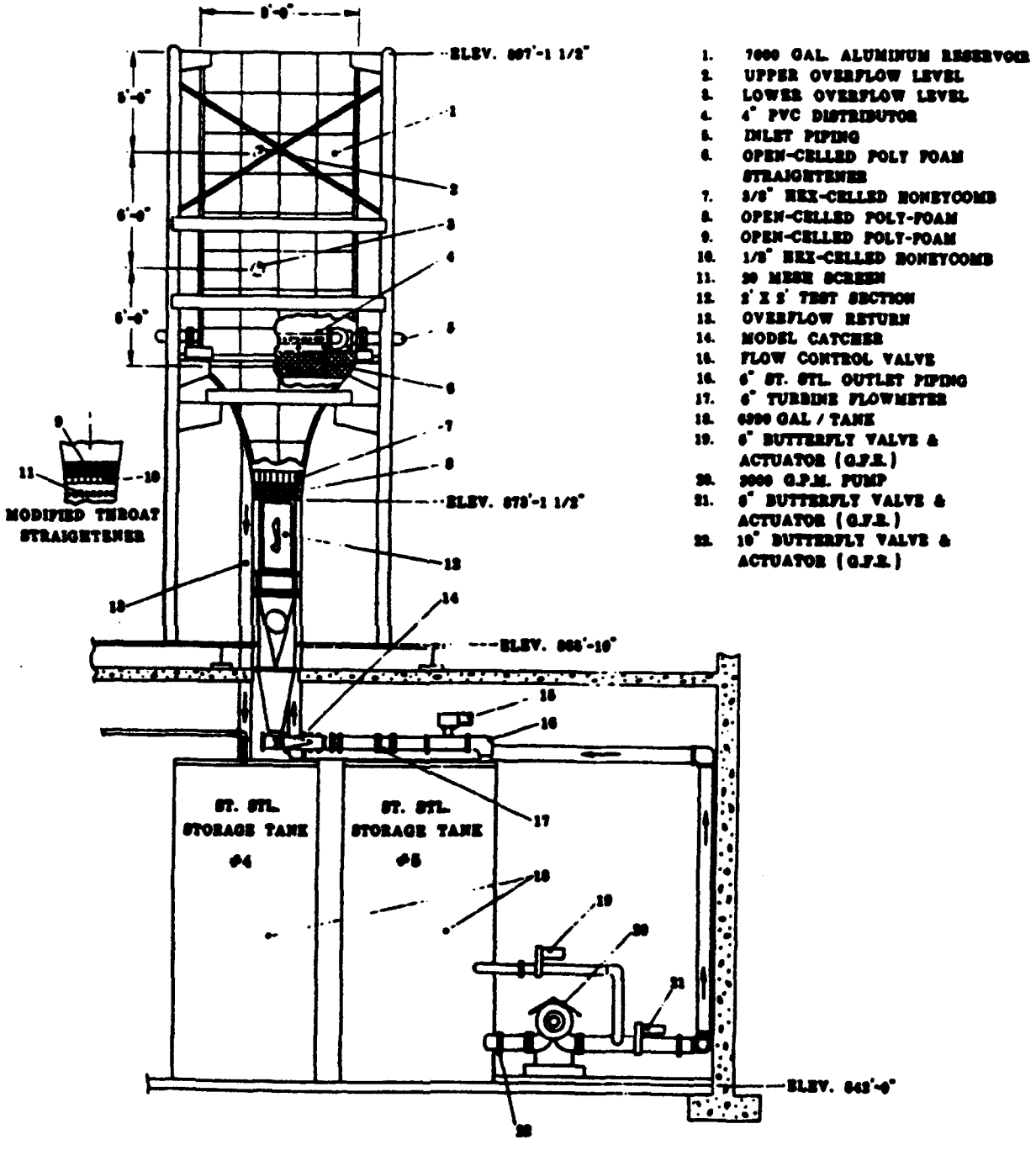

Figure 1 Hydrodynamic Facility

Run	α	β	Canard α
1	+5, +40	0	Off
2	"	+5	Off
3	"	0	Off
4	"	0	+10
5	"	0	0
6	"	0	-10
7	"	0	-20
8	+5, +40	+10	-10
9	18	+10	-10
10	18	-5	-10
11	18	0	-10
12	15	+10	-10
13	15	+5	-10
14	15	0	-10
15	+5, +40	-5	-10

Figure 2 ATTAC Water Tunnel Test Matrix

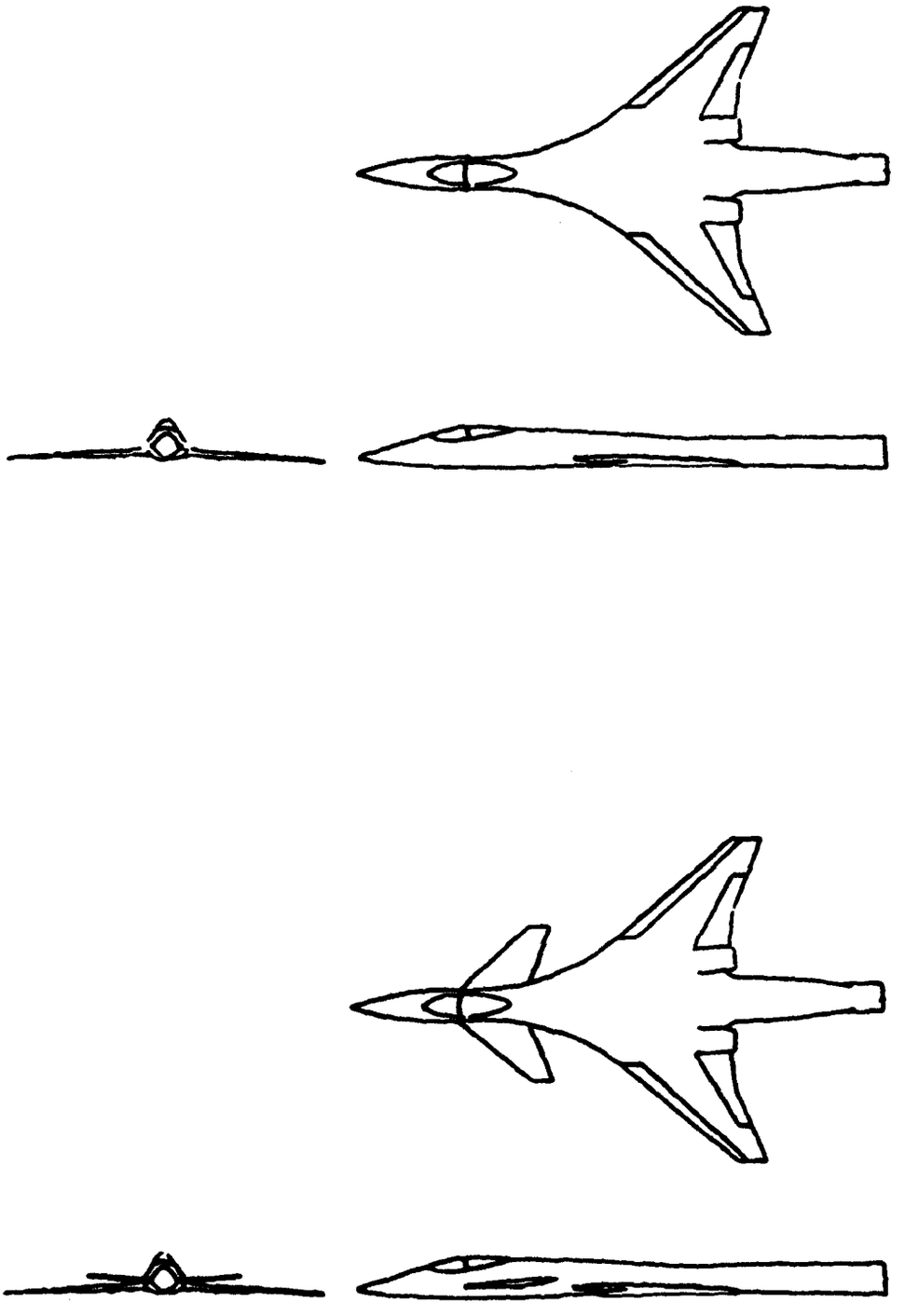

Figure 3 ATTAC Water Tunnel Test Configuration

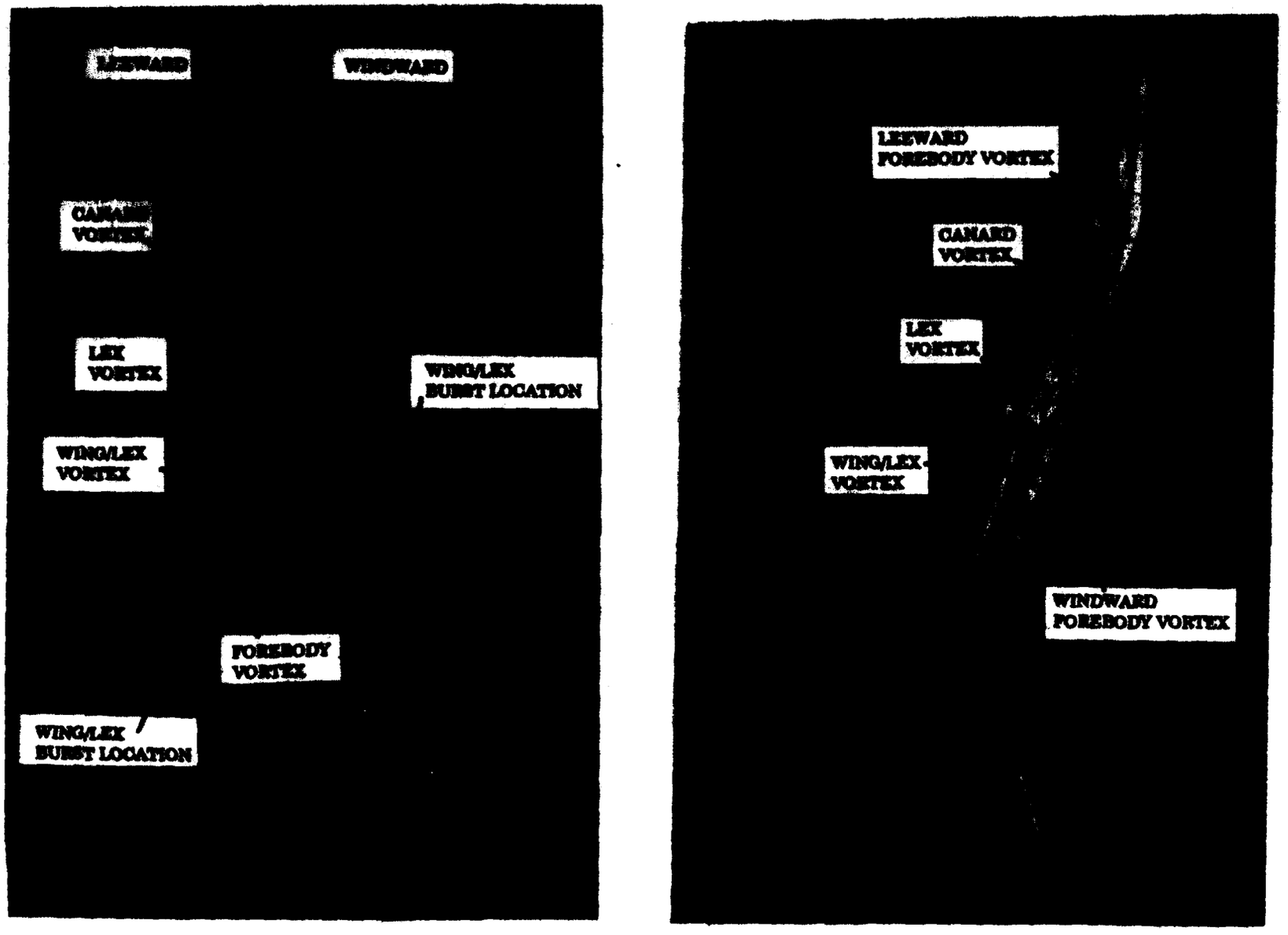

Figure 4 ATTAC Vortex System Identification

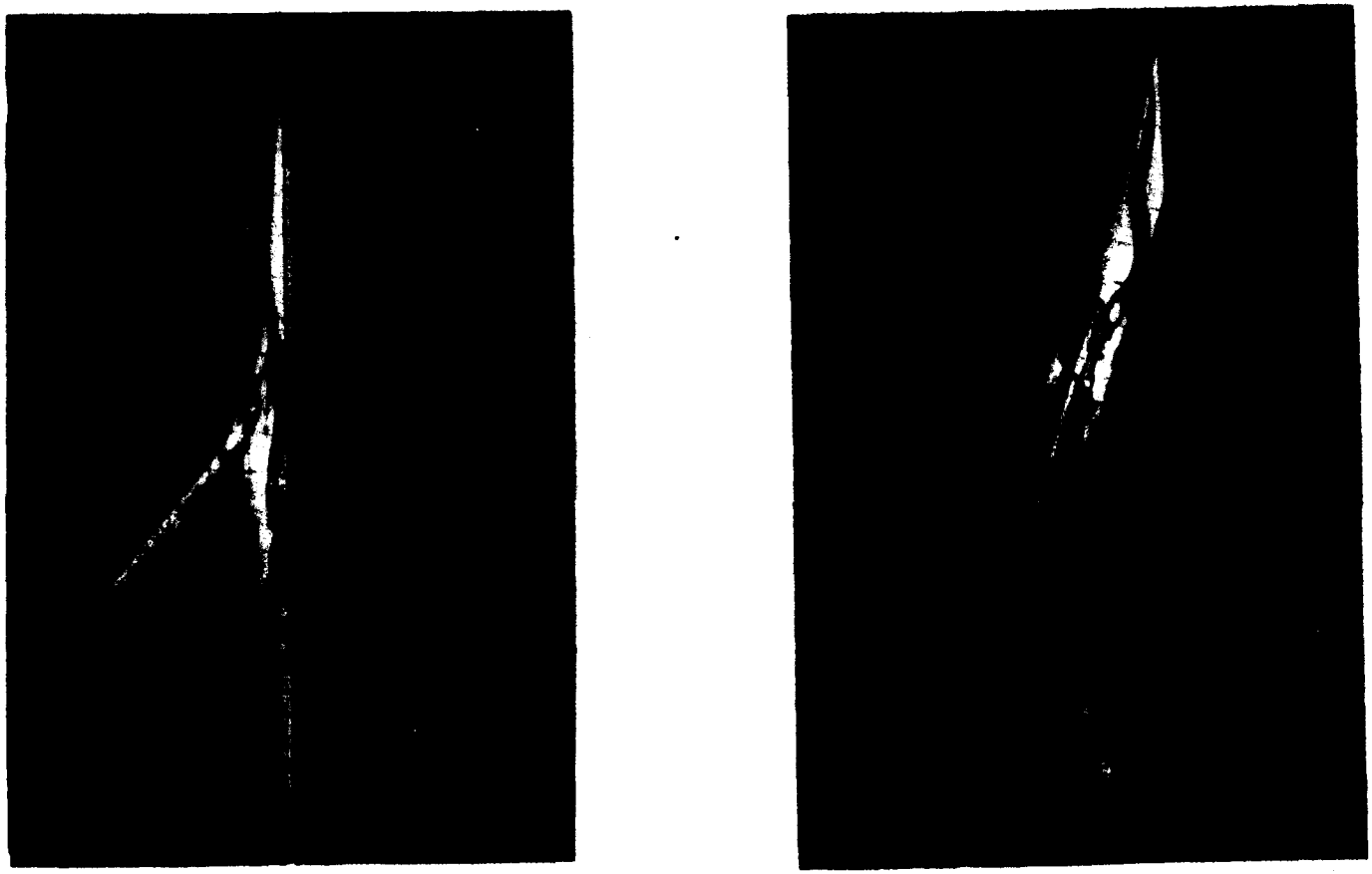

Figure 5 $\alpha = 15^{o}; \beta = 0^{o}; \alpha_c = \text{Off}$

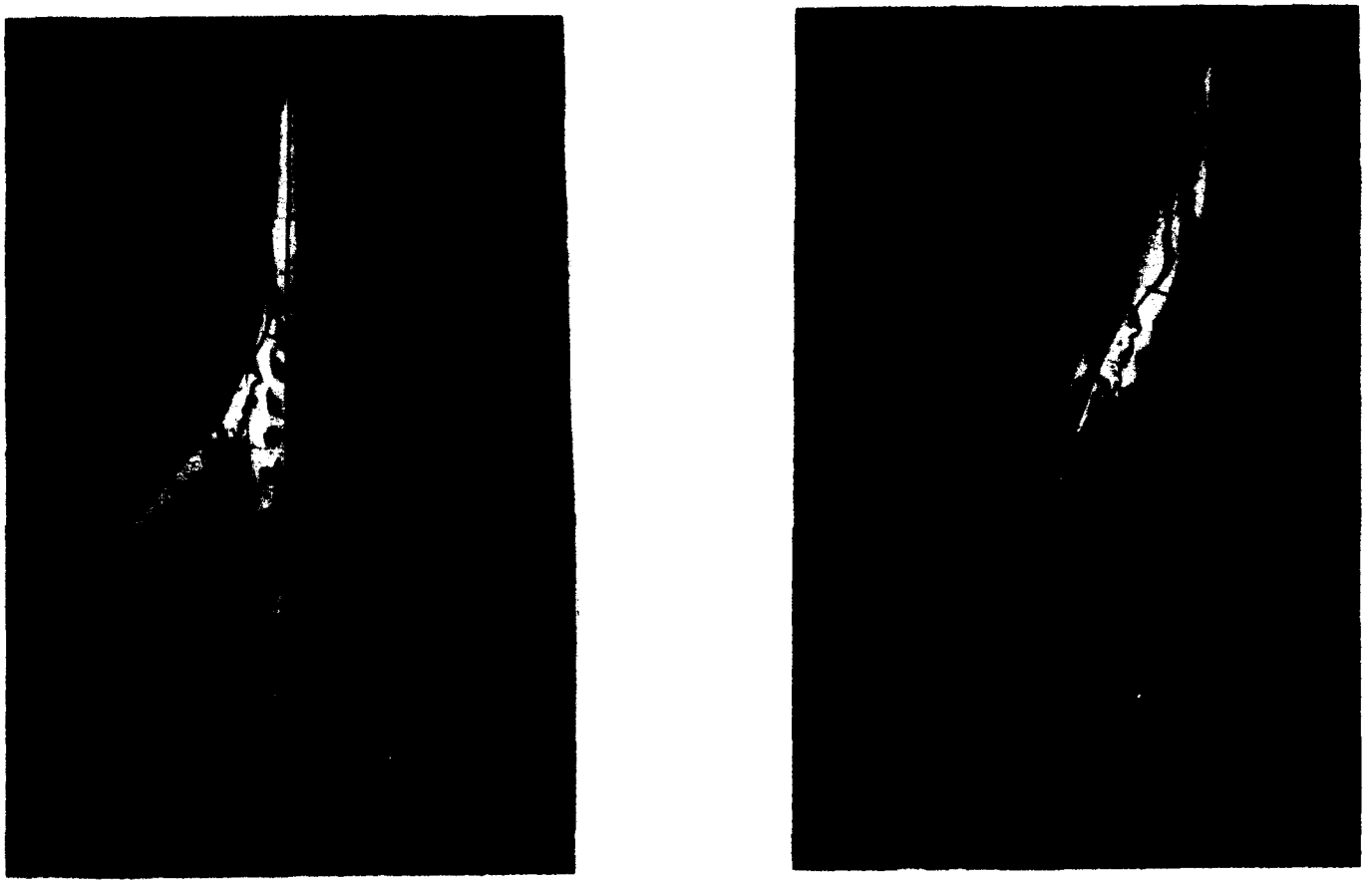

Figure 6 $\alpha = 20^{o}$; $\beta = 0^{o}$; α_c = Off

Figure 7 $\alpha = 35^{o}$; $\beta = 0^{o}$; α_c = Off

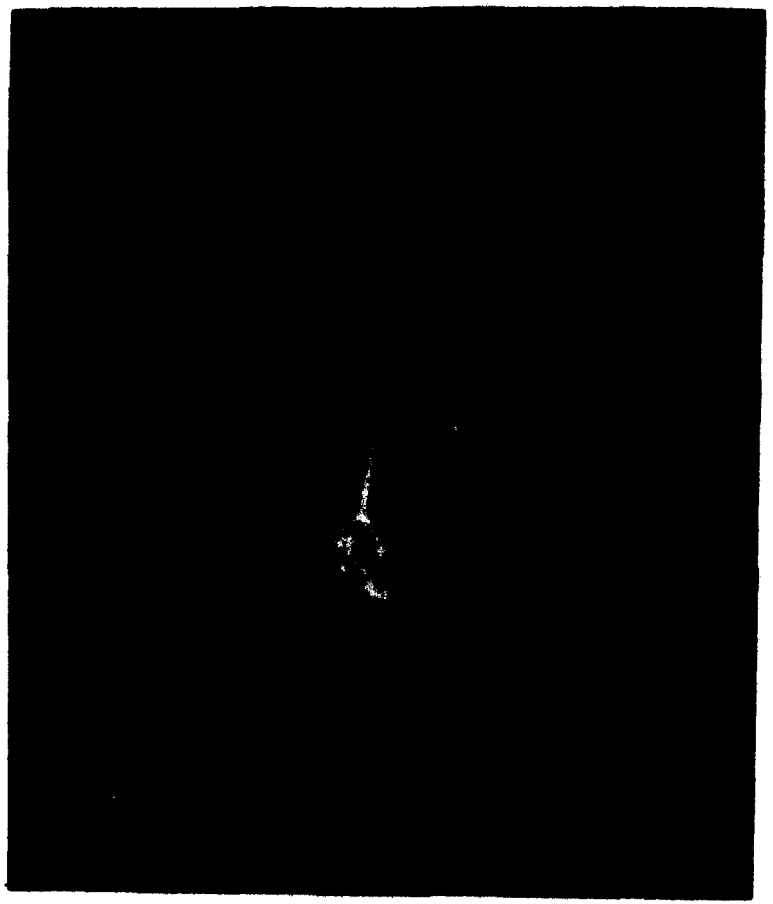

Figure 8 $\alpha = 40^{o}; \beta = 0^{o};$ (reference 4)

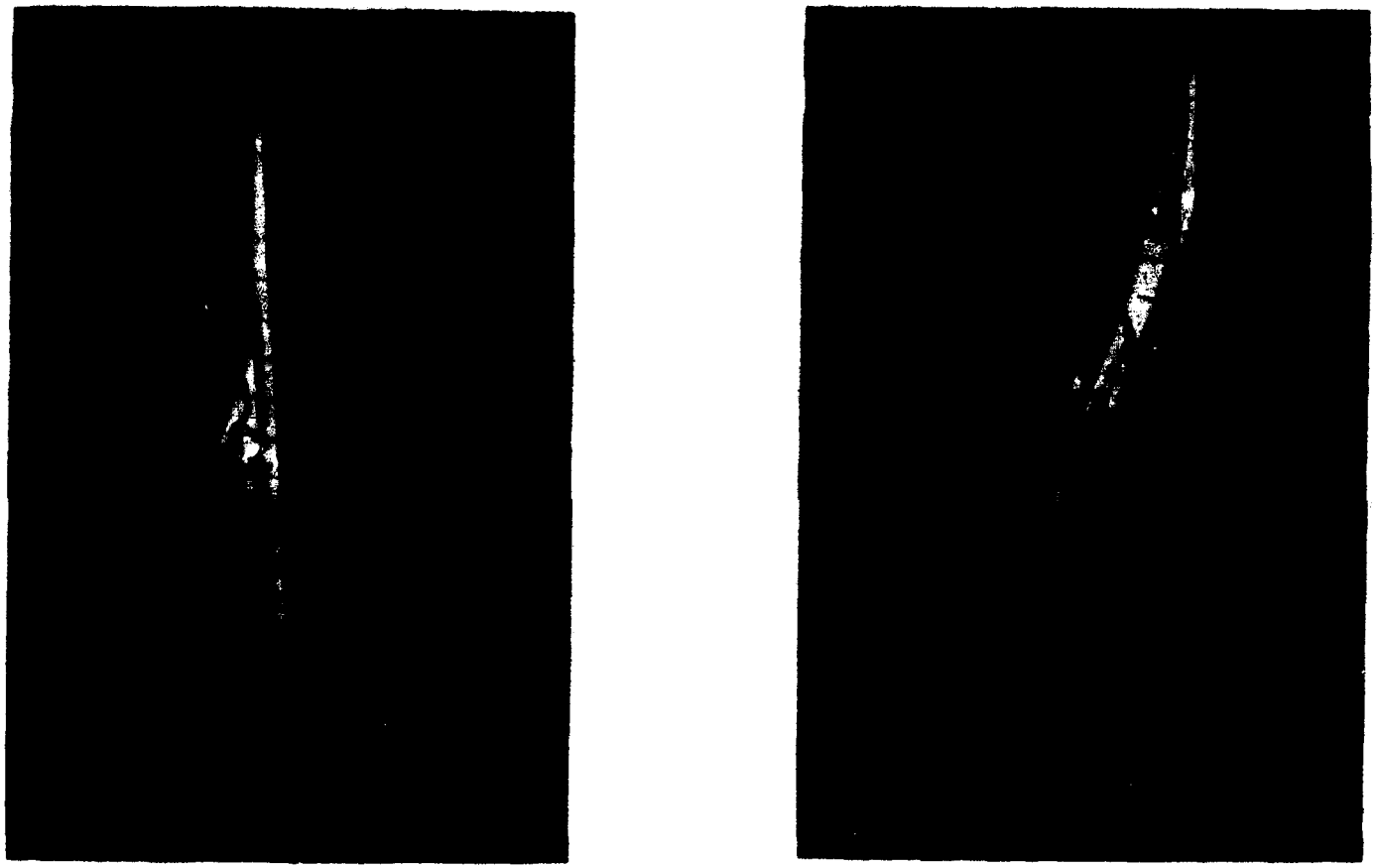

Figure 9 $\alpha = 15^{o}$; $\beta = 45^{o}$; α_c = Off

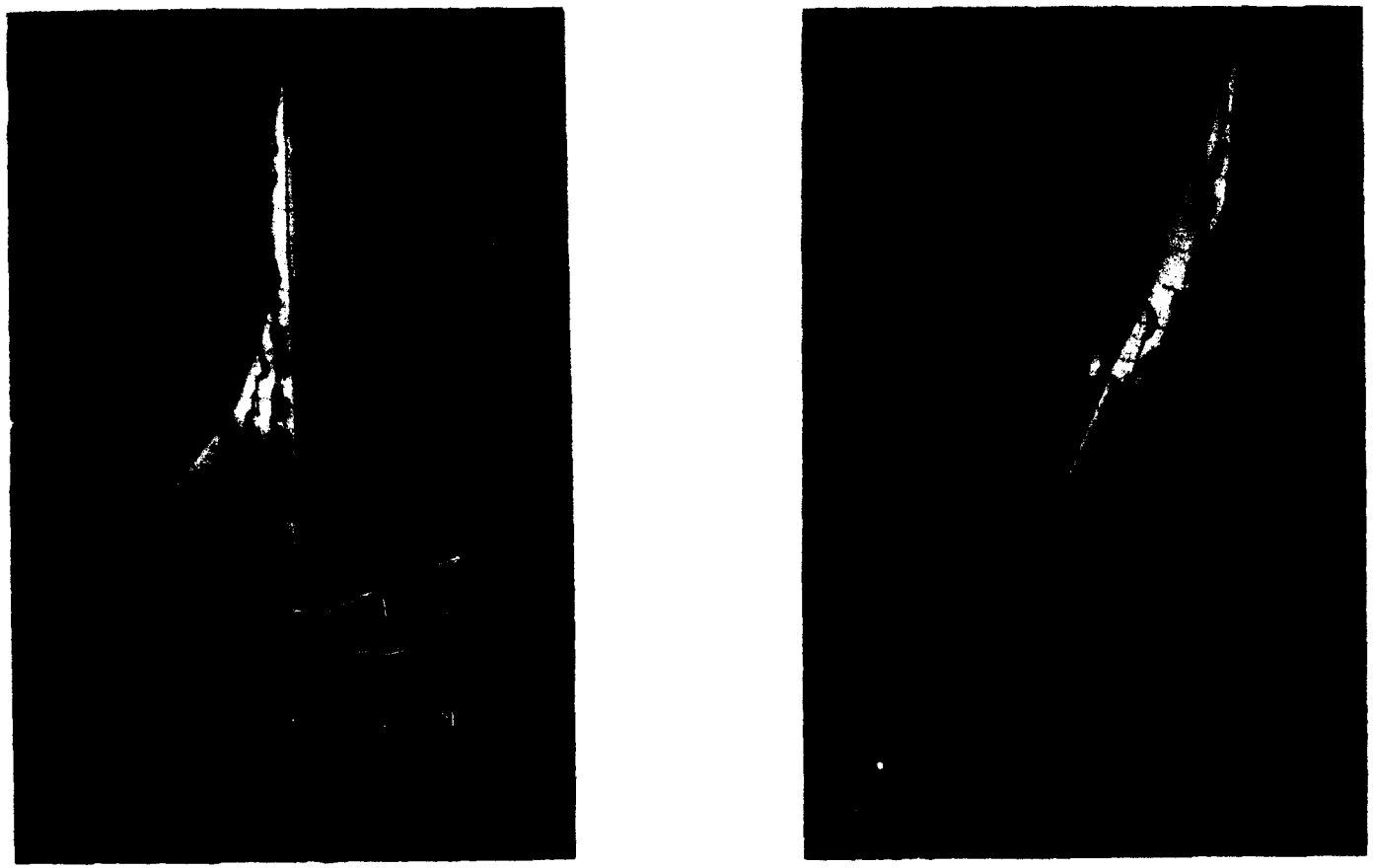

Figure 10 $\alpha = 20^{o}$; $\beta = \pm 5^{o}$; α_c = Off

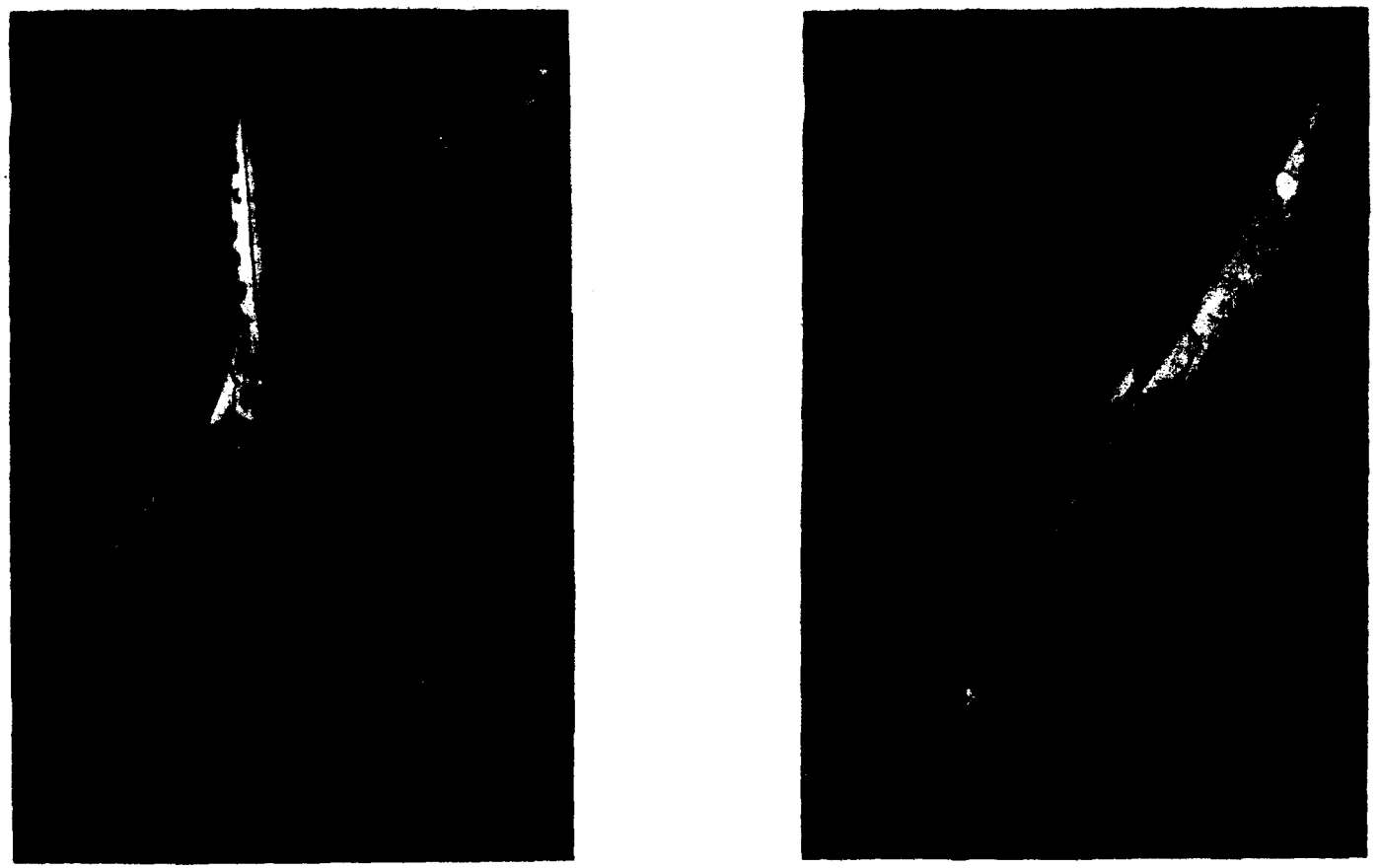

Figure 11 $\alpha = 30^{o}$; $\beta = +5^{o}$; α_c = Off

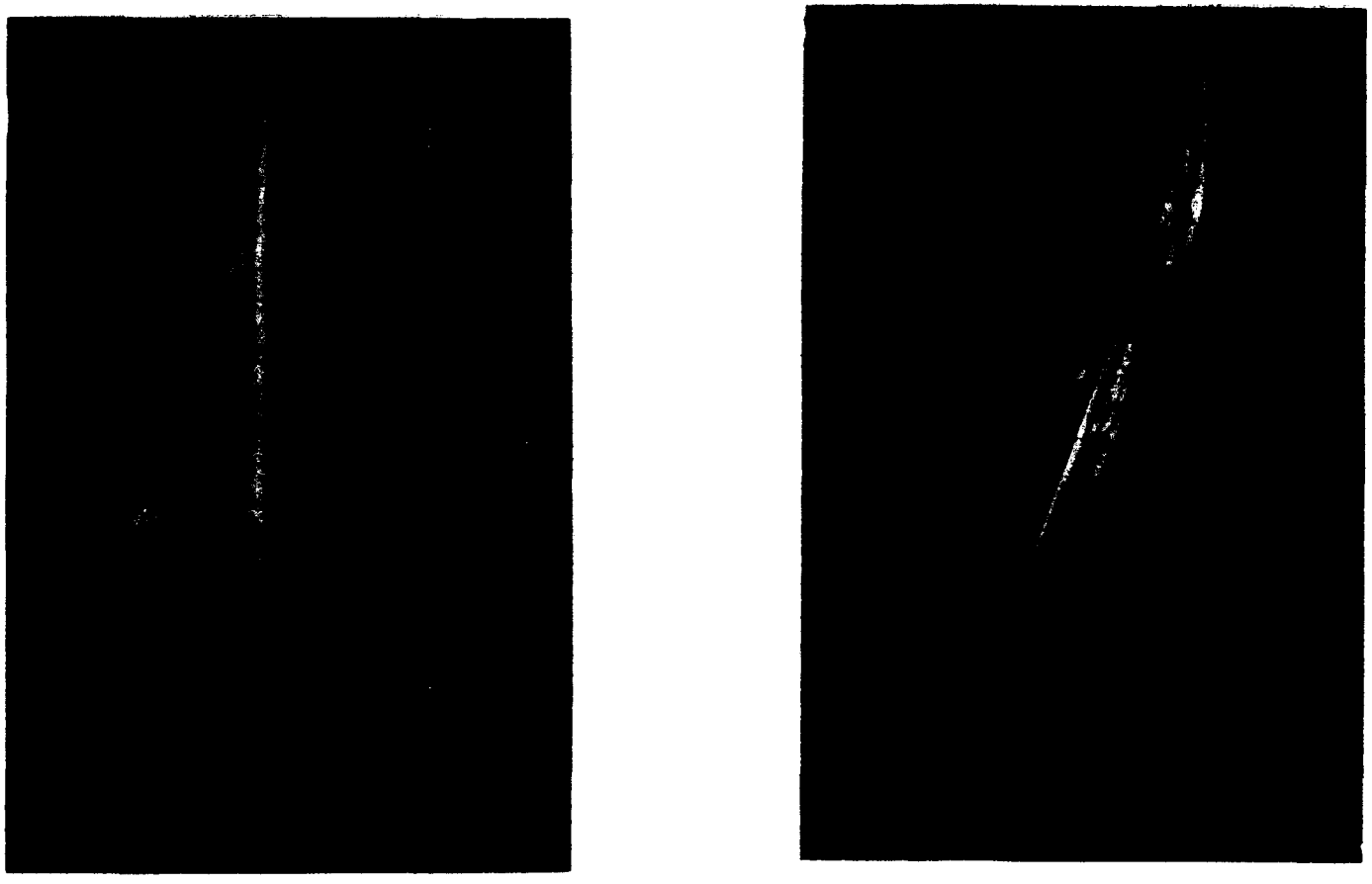

Figure 12 $\alpha = 15^{o}; \beta = 0^{o}; \alpha_c = 0^{o}$

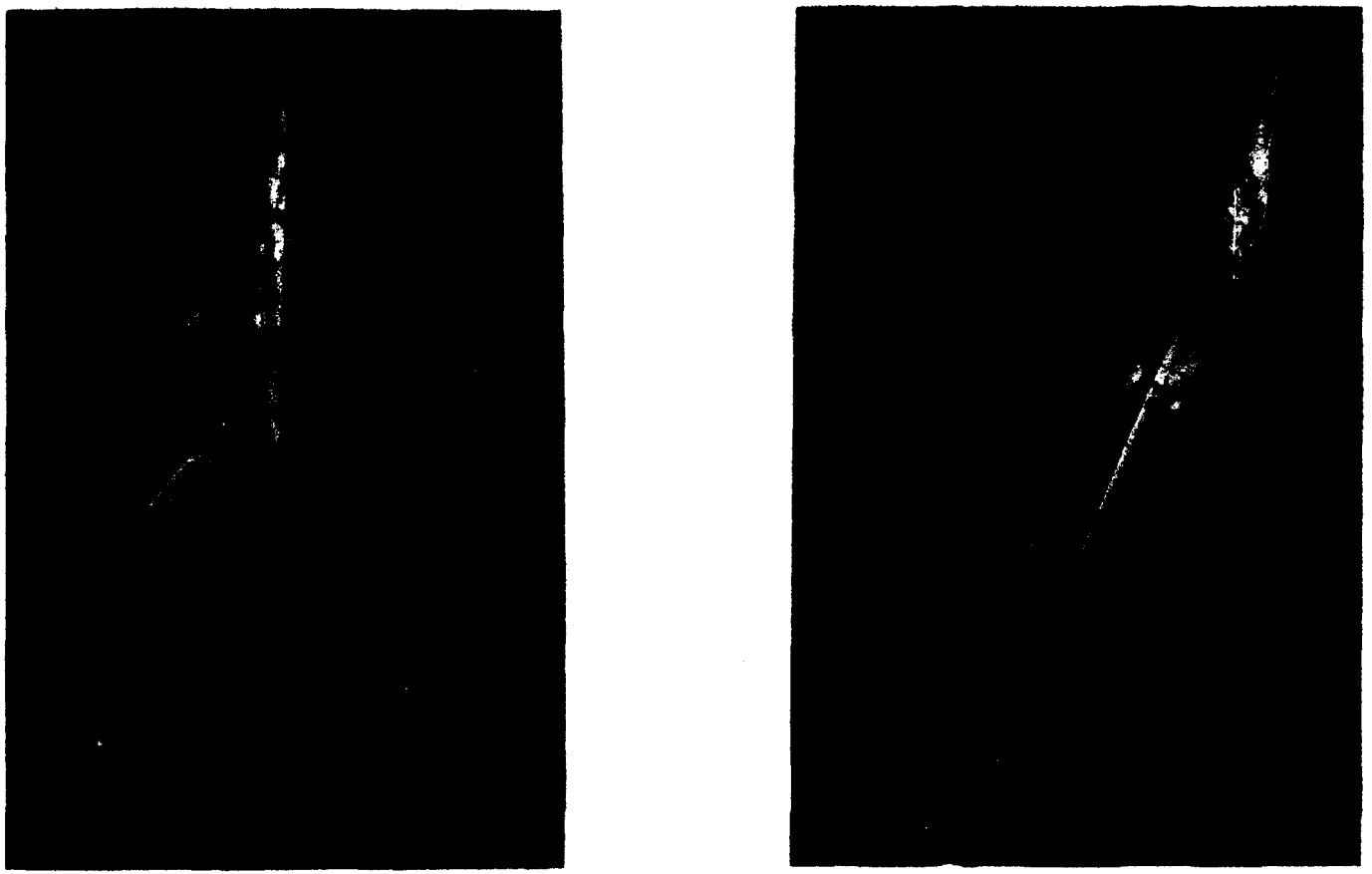

Figure 13 $\alpha = 20^o$; $\beta = 0^o$; $\alpha_c = 0^o$

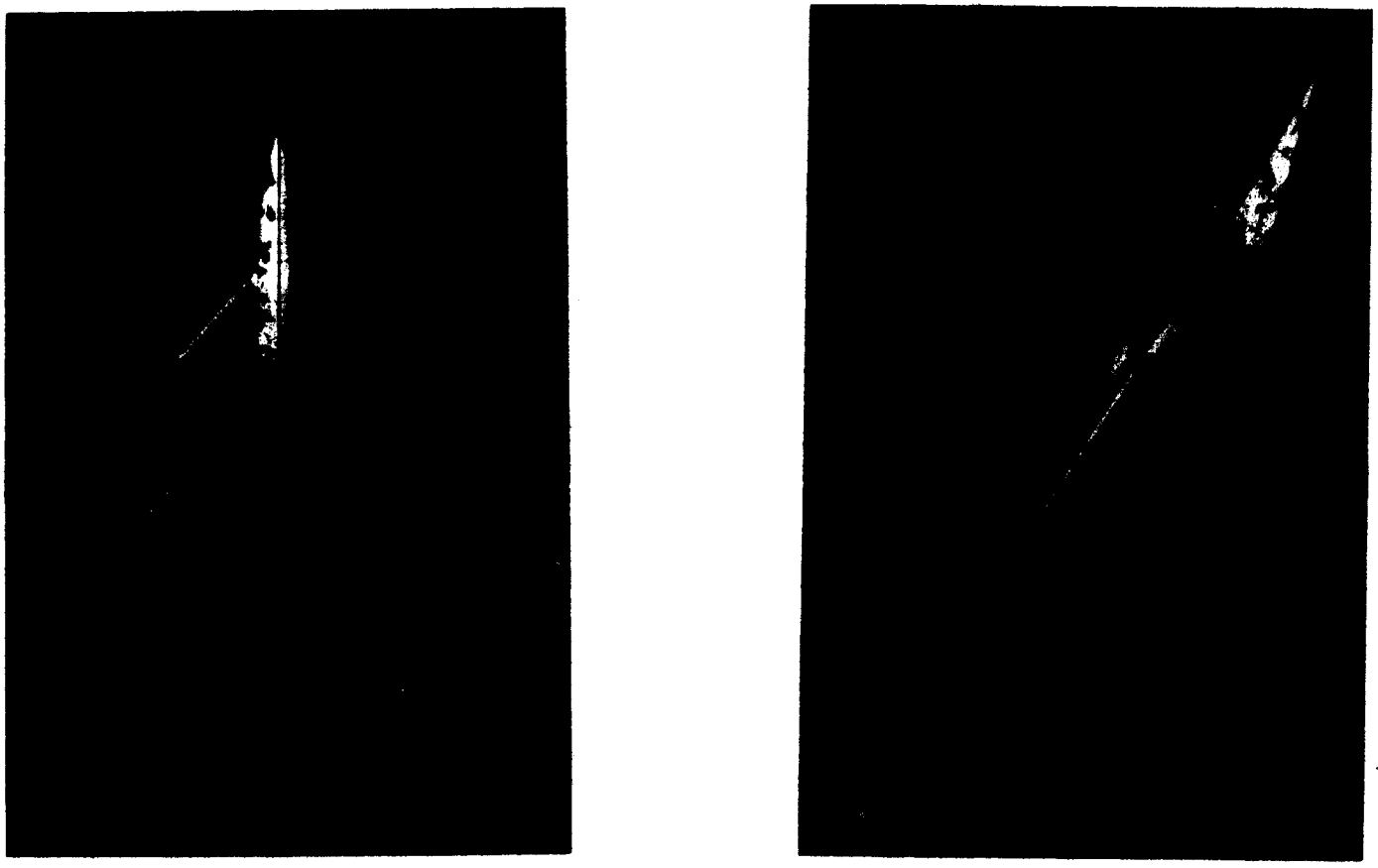

Figure 14 $\alpha = 30^{o}$; $\beta = 0^{o}$; $\alpha_c = 0^{o}$

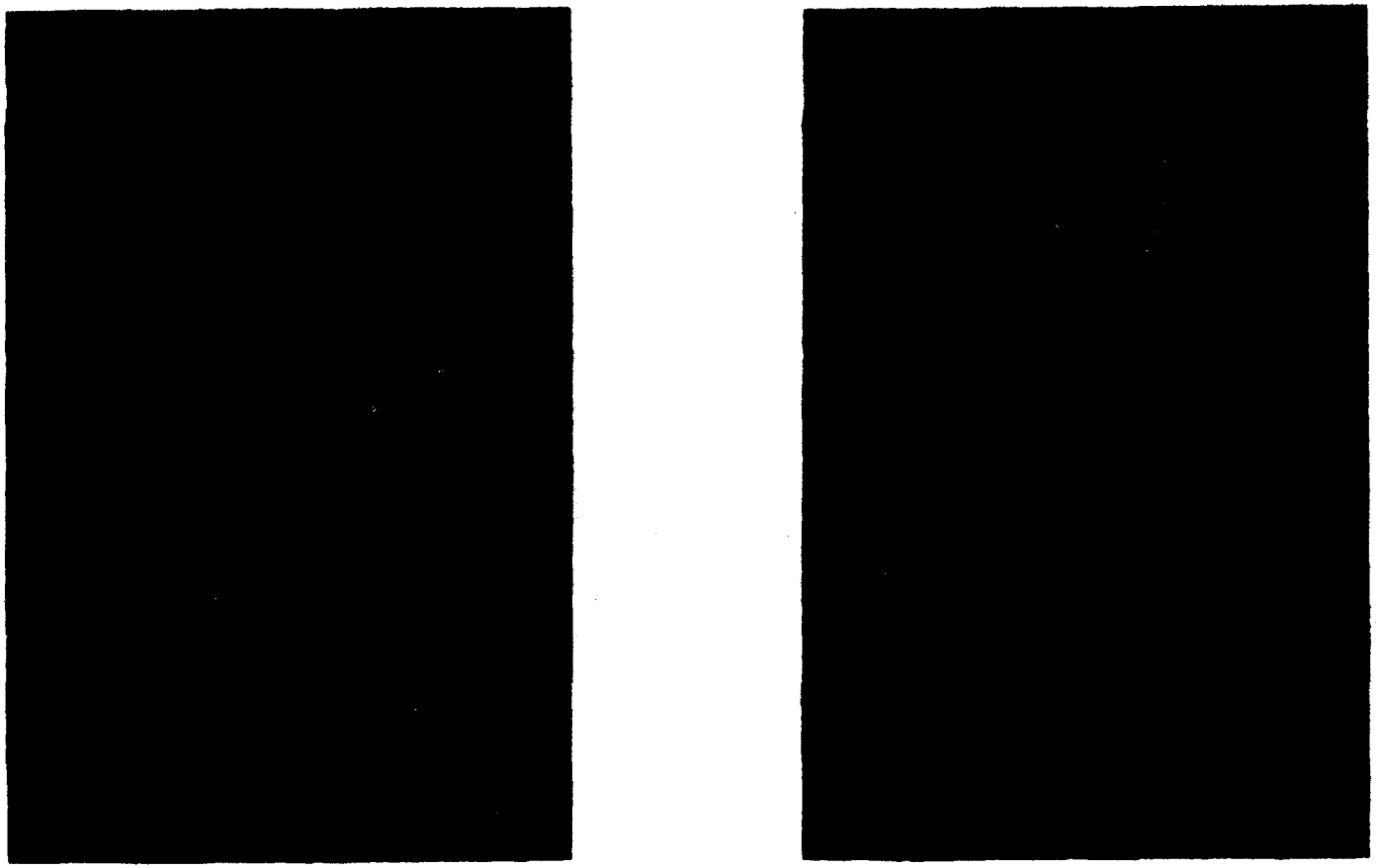

Figure 15 $\alpha = 15^o; \beta = 0^o; \alpha_c = -10^o$

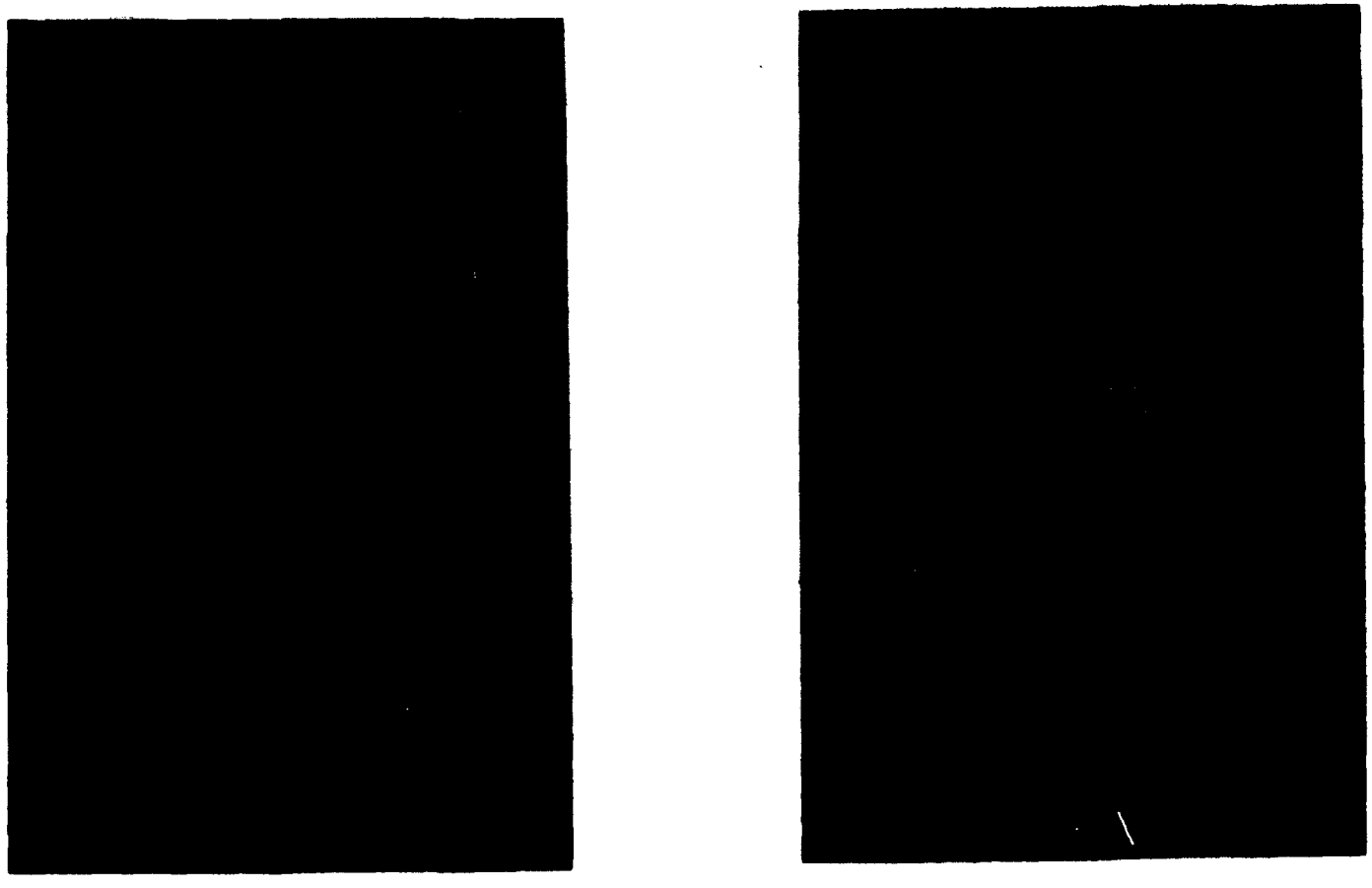

Figure 16 $\alpha = 18^{o}; \beta = 0^{o}; \alpha_{c} = -10^{o}$

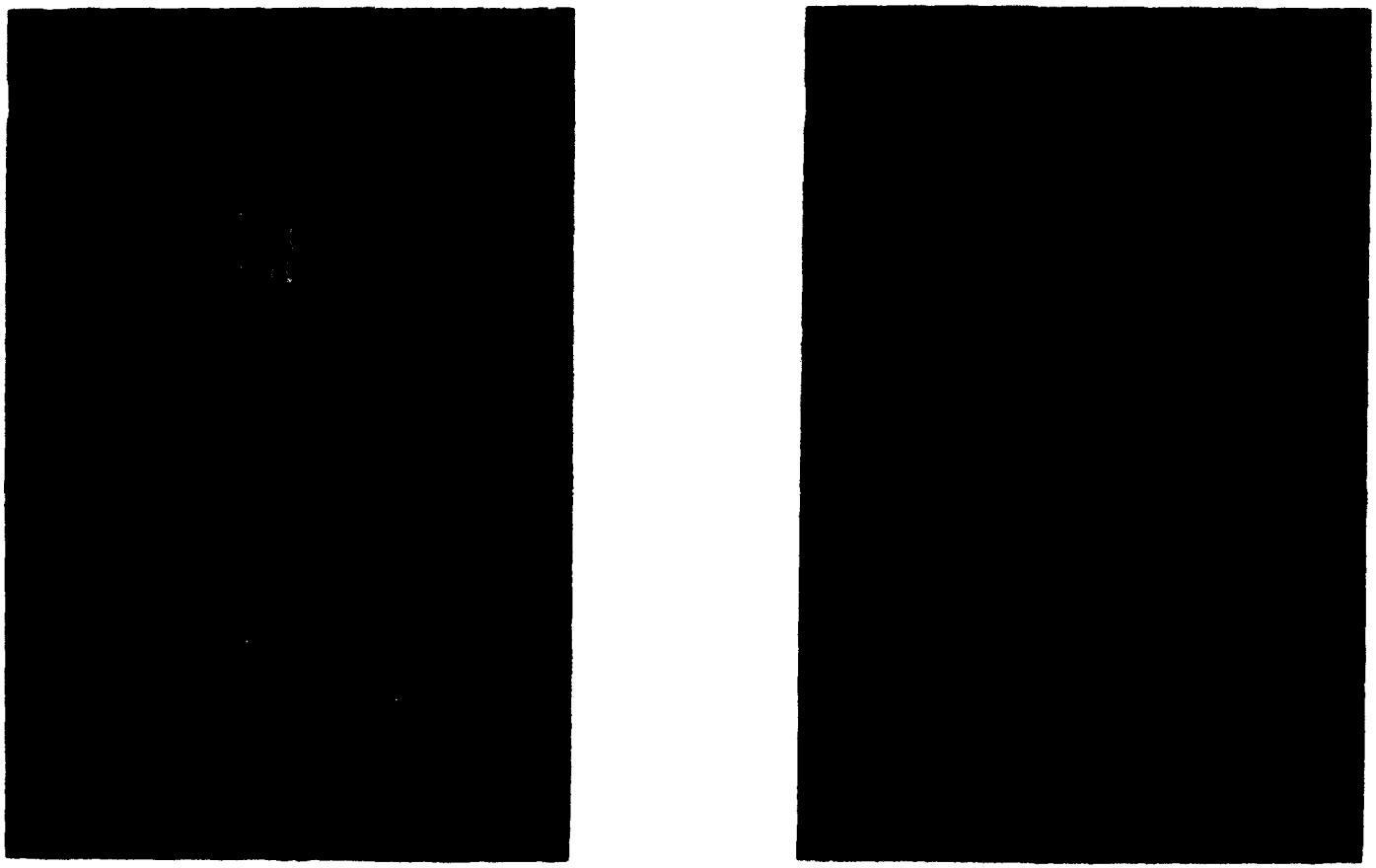

Figure 17 $\alpha = 25^{o}; \beta = 0^{o}; \alpha_c = -10^{o}$

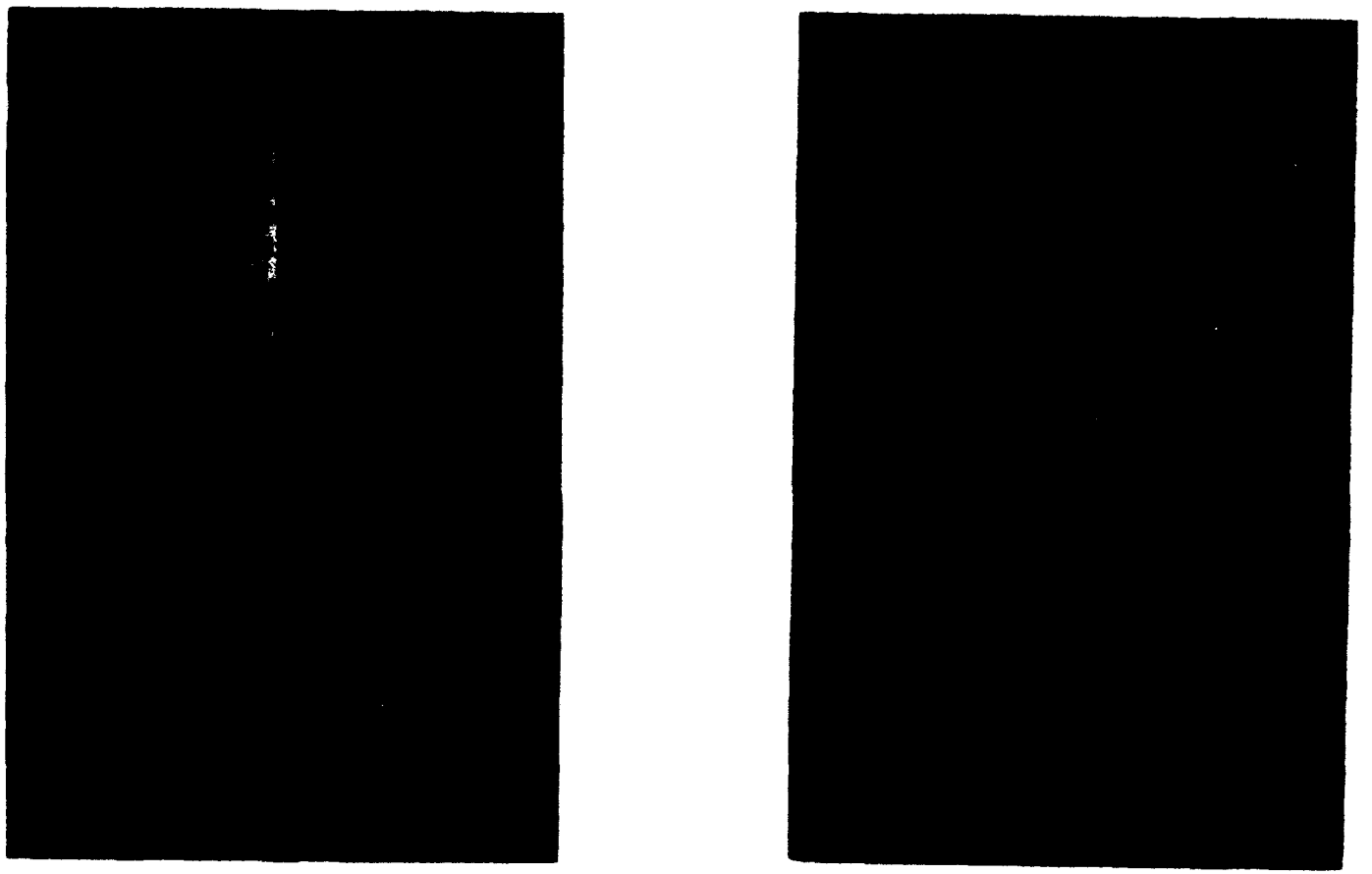

Figure 18 $\alpha = 35^{o}; \beta = 0^{o}; \alpha_{c} = -10^{o}$

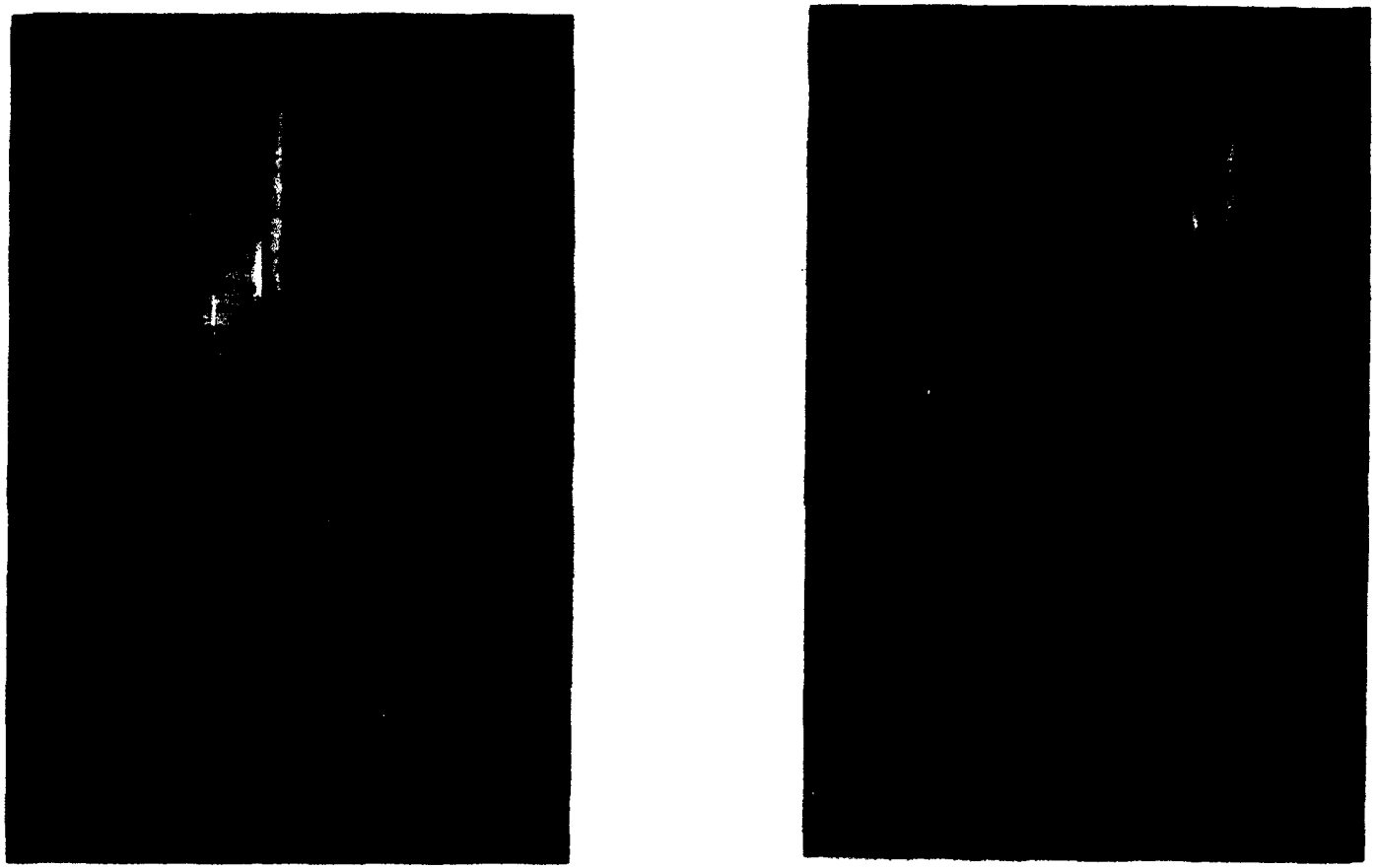

Figure 19 $\alpha = 15^{o}; \beta = 0^{o}; \alpha_{c} = -20^{o}$

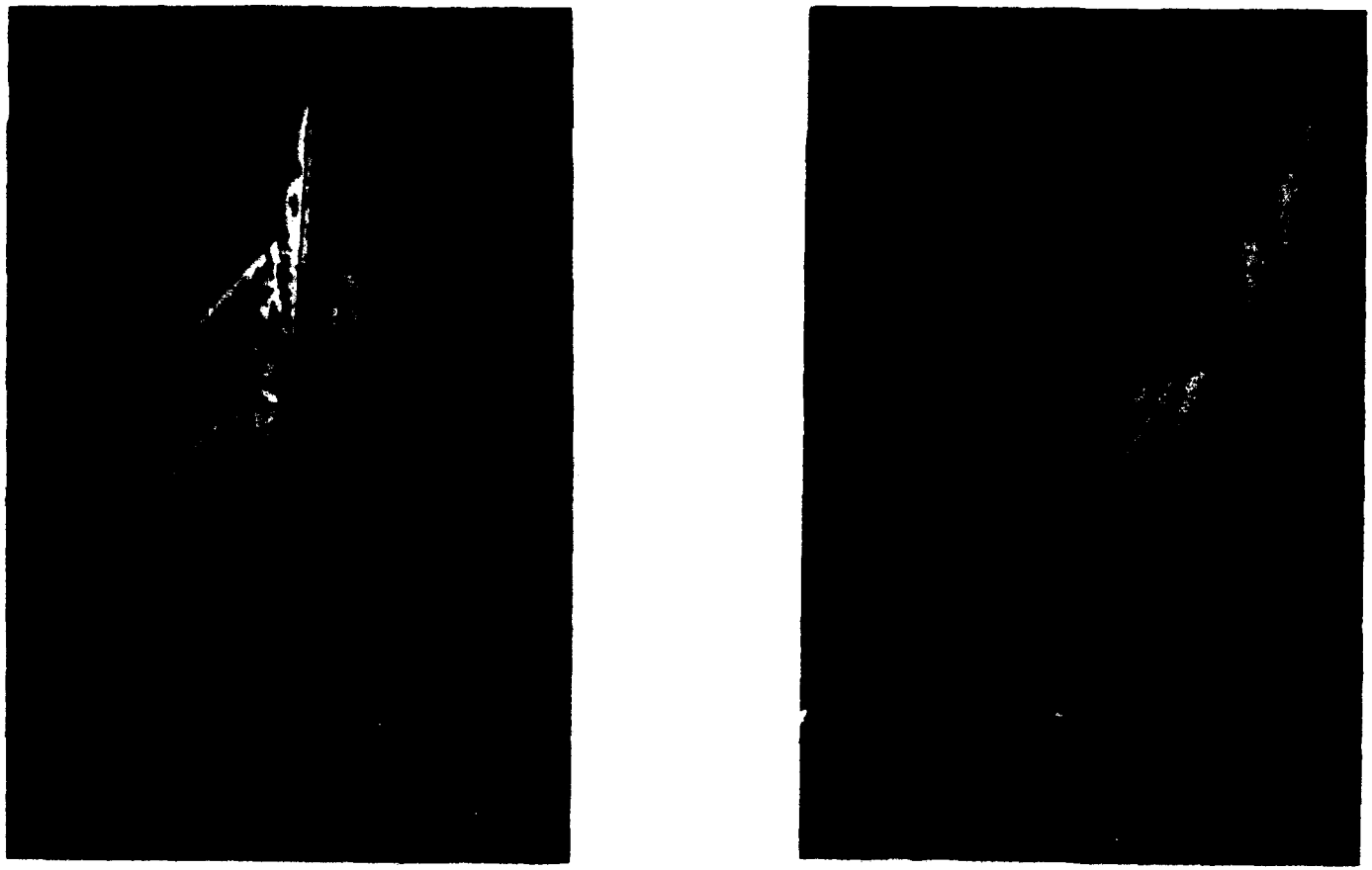

Figure 20 $\alpha = 25^o$; $\beta = 0^o$; $\alpha_c = -20^o$

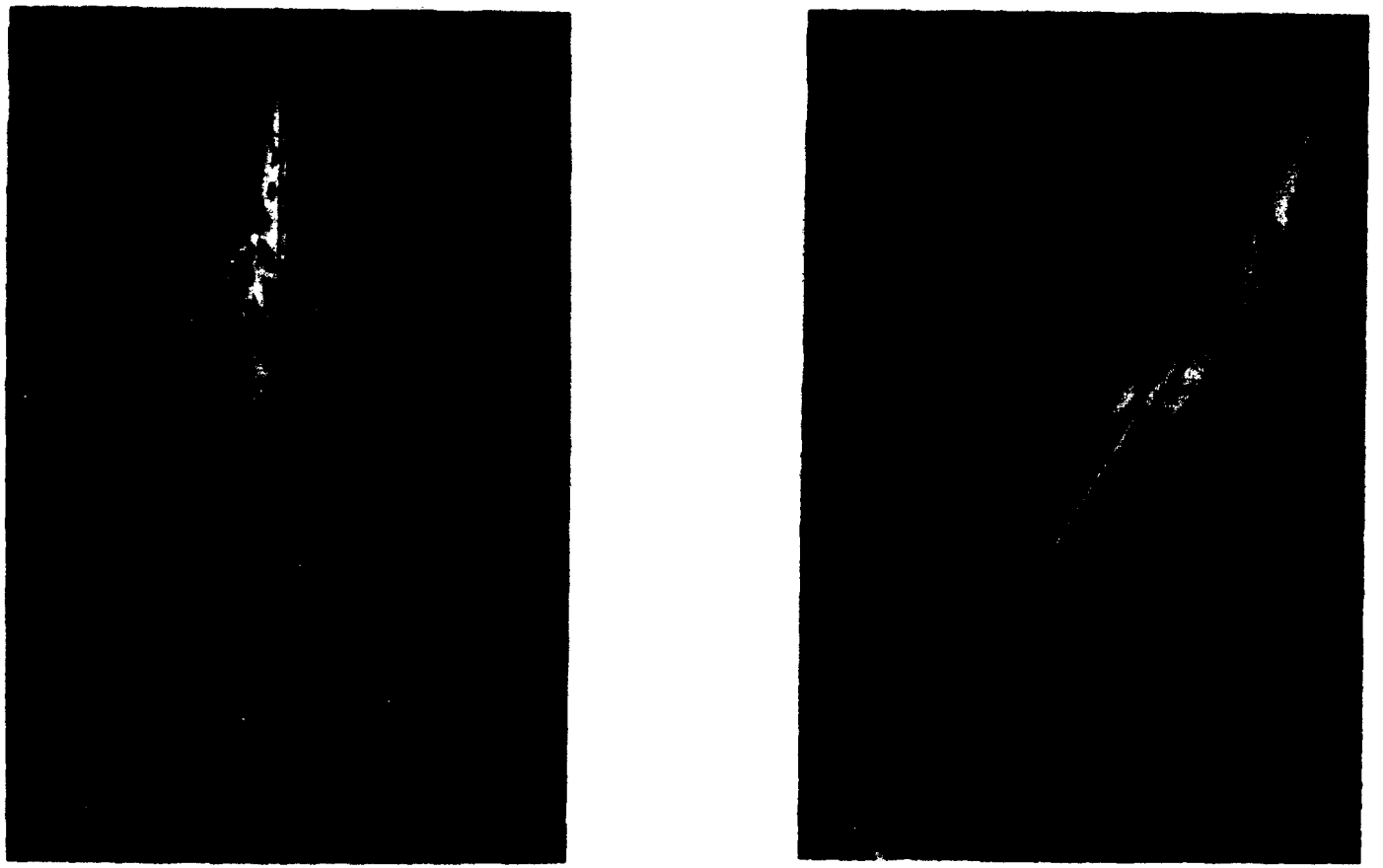

Figure 21 $\alpha = 30^{o}$; $\beta = 0^{o}$; $\alpha_c = -20^{o}$

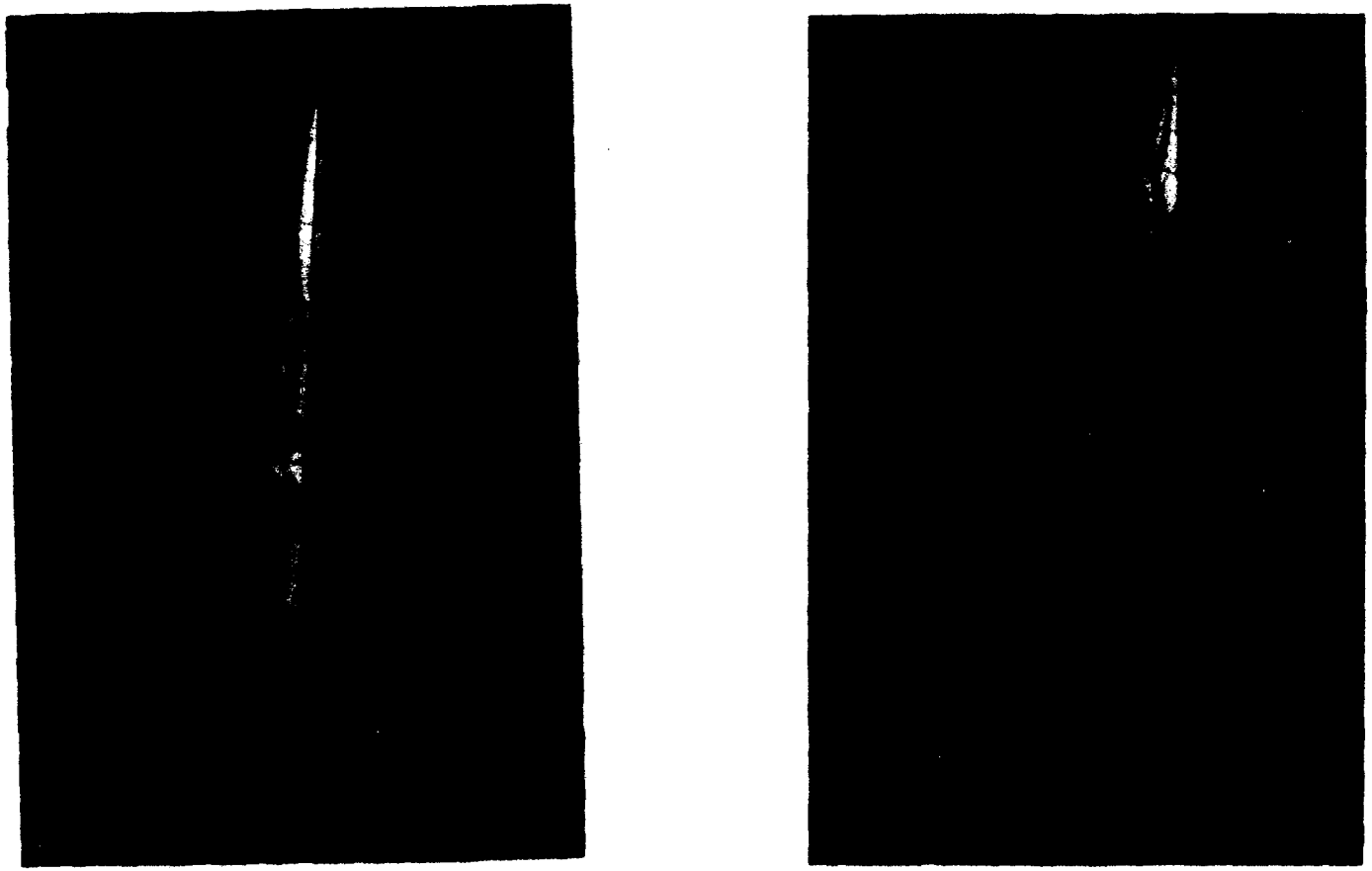

Figure 22 $\alpha = 15^{o}; \beta = 0^{o}; \alpha_c = +10^{o}$

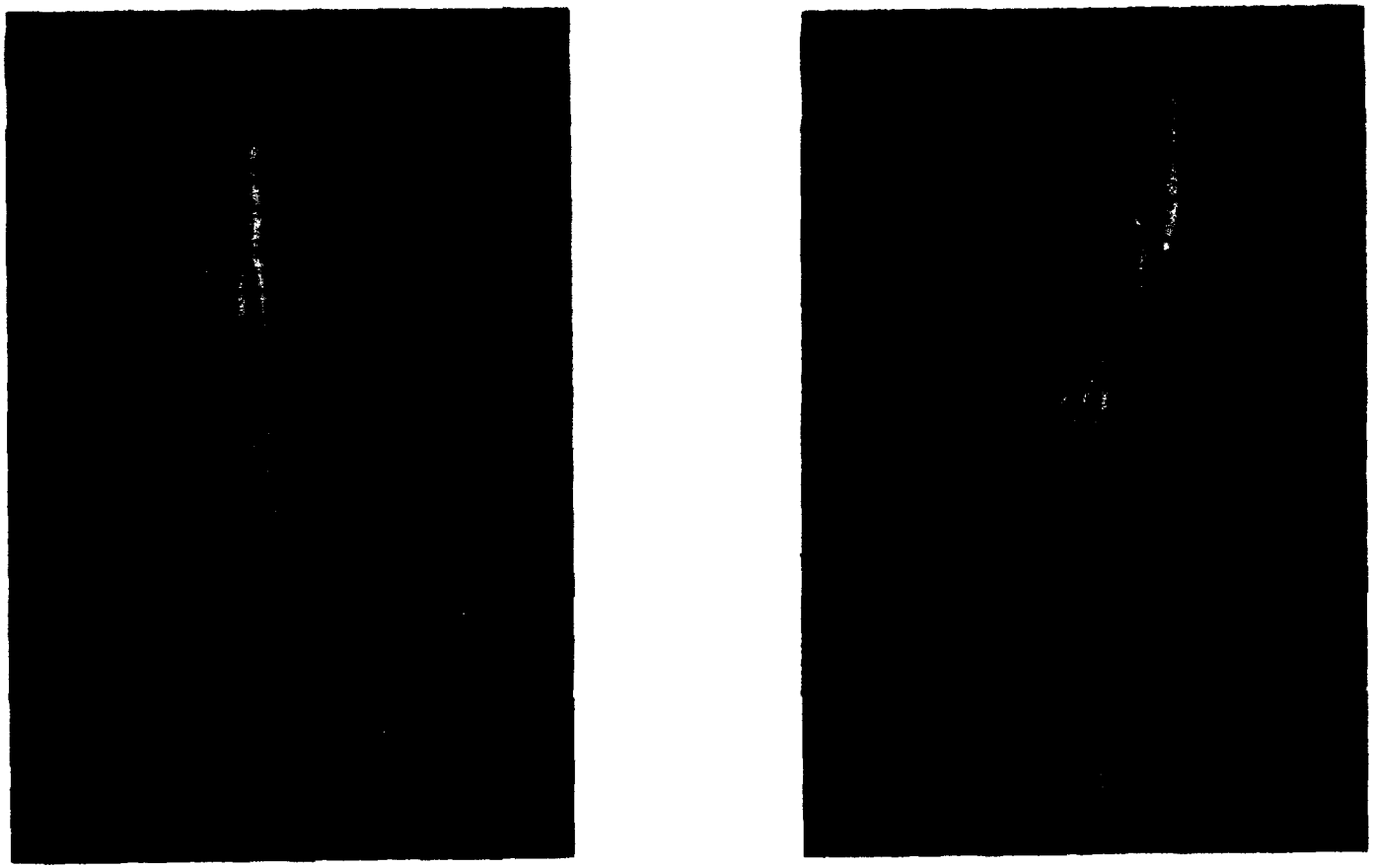

Figure 23 $\alpha = 15^{o}; \beta = +5^{o}; \alpha_c = -10^{o}$

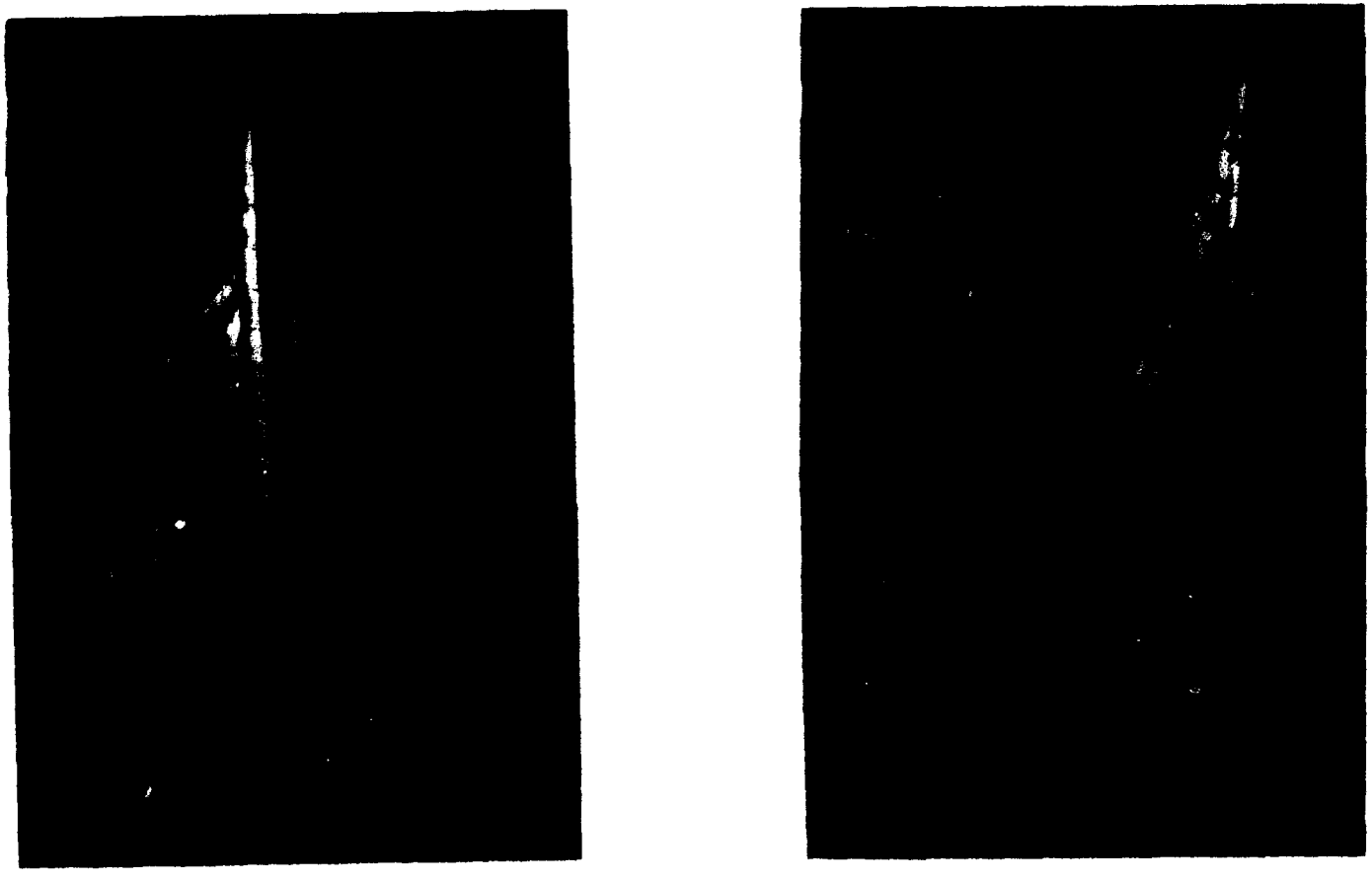

Figure 24 $\alpha = 20^{o}$; $\beta = \pm 5^{o}$; $\alpha_c = -10^{o}$

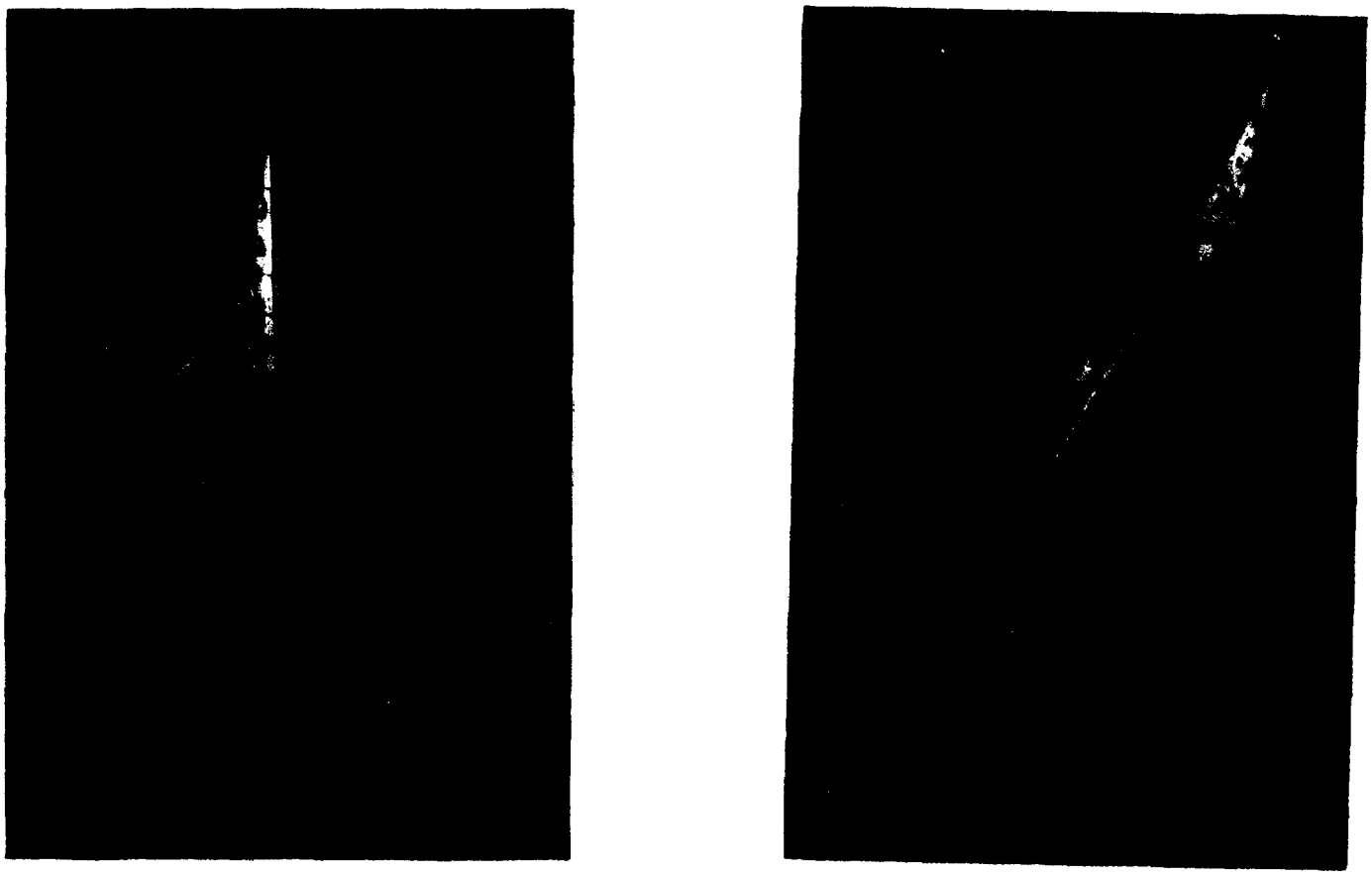

Figure 25 $\alpha = 30^{o}$; $\beta = +5^{o}$; $\alpha_c = -10^{o}$

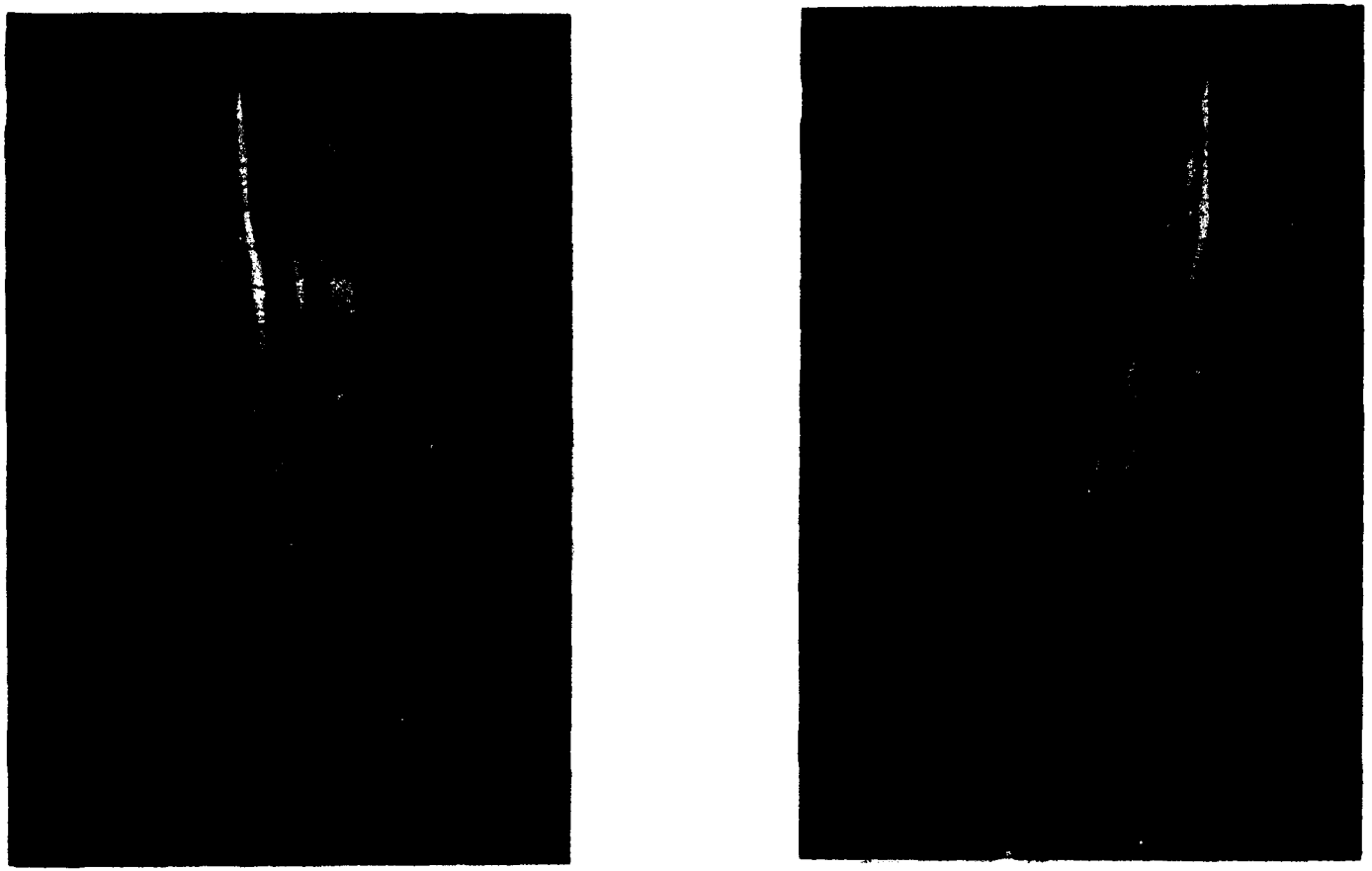

Figure 26 $\alpha = 15^{o}$; $\beta = +10^{o}$; $\alpha_c = -10^{o}$

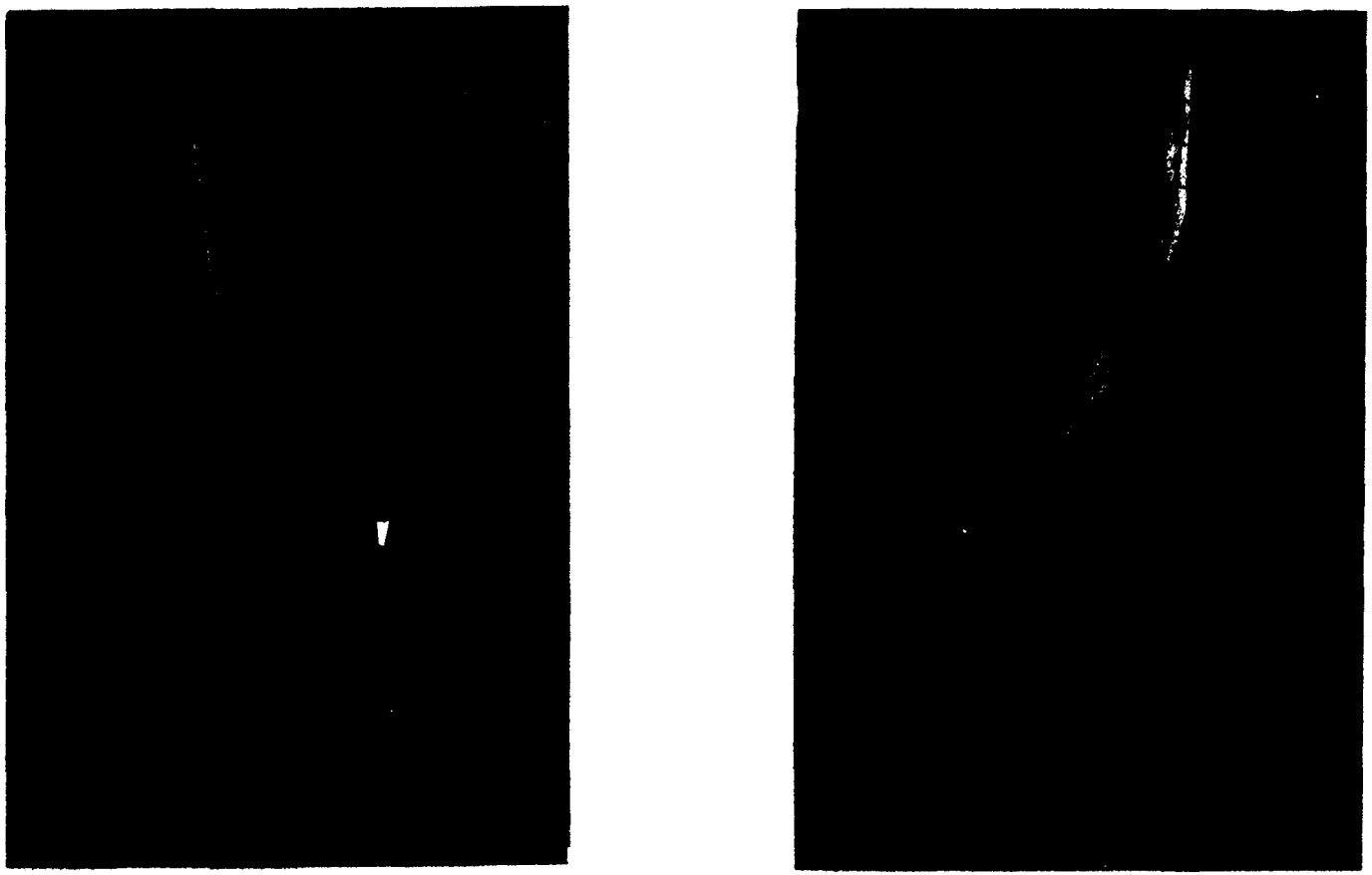

Figure 27 $\alpha = 18^{o}$; $\beta = +10^{o}$; $\alpha_c = -10^{o}$

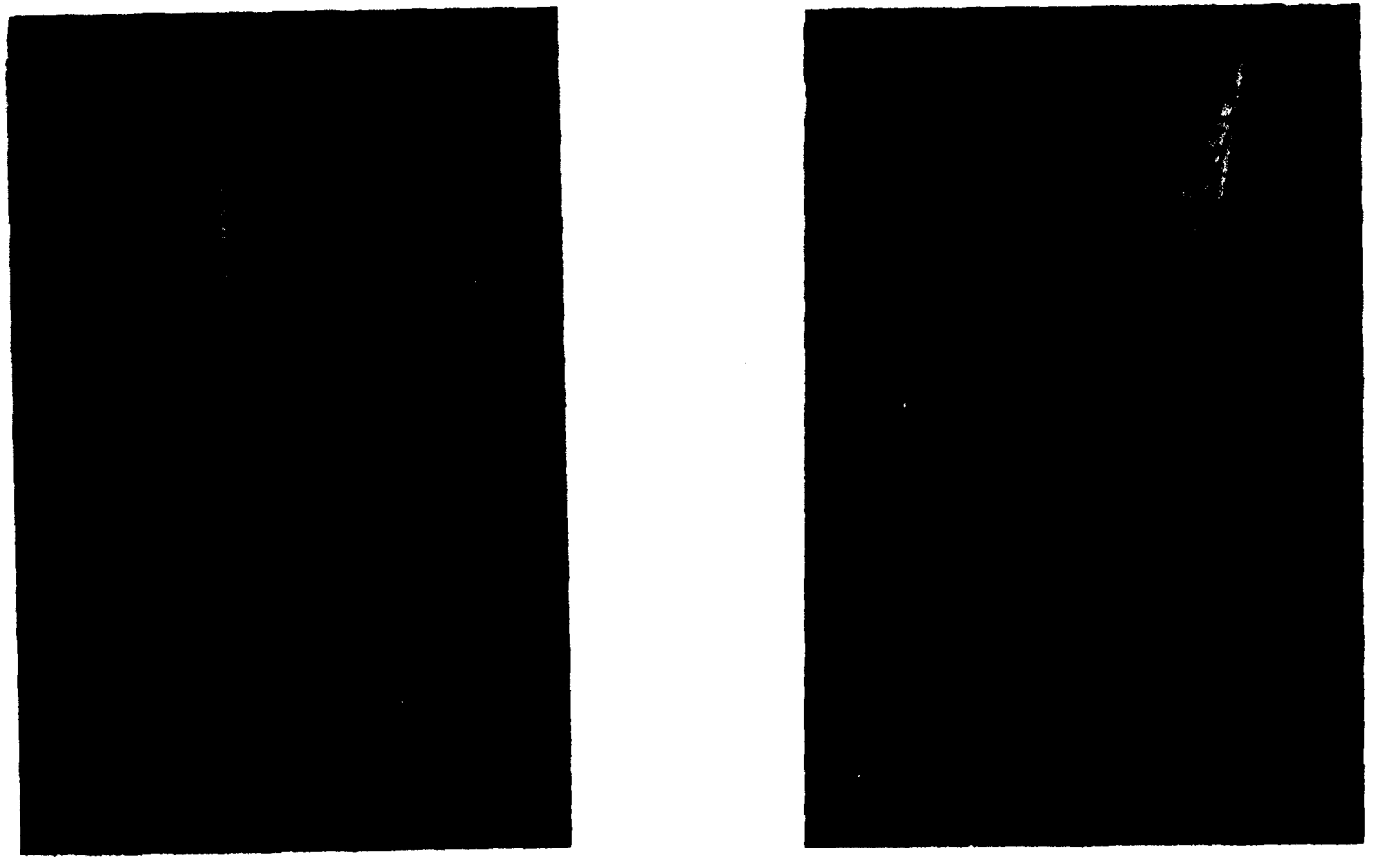

Figure 28 $\alpha = 25^{o}$; $\beta = +10^{o}$; $\alpha_c = -10^{o}$

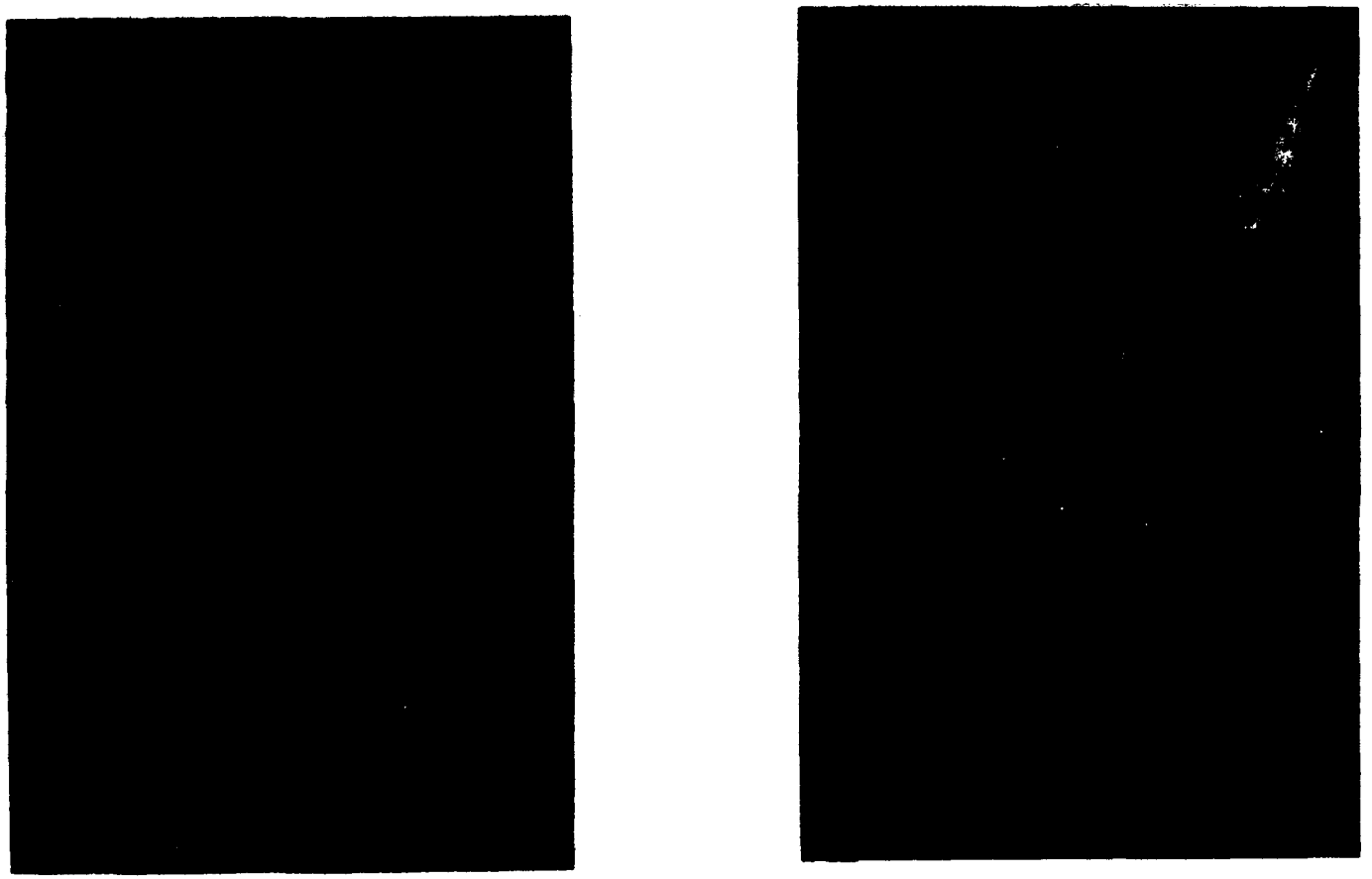

Figure 29 $\alpha = 30^{o}$; $\beta = +10^{o}$; $\alpha_c = -10^{o}$